THE PENNSYLVANIA STATE UNIVERSITY
SCHREYER HONORS COLLEGE

DEPARTMENT OF BIOCHEMISTRY & MOLECULAR BIOLOGY

Understanding the Mechanisms Controlling the Localization of Microtubule Organization Proteins in *Drosophila* Neurons

MELISSA LONG
SPRING 2022

A thesis
submitted in partial fulfillment
of the requirements
for a baccalaureate degree
in Immunology and Infectious Disease
with honors in Biochemistry & Molecular Biology

Reviewed and approved* by the following:

Melissa Rolls
Chair, Intercollege Graduate Degree Program in Molecular, Cellular and Integrative Biosciences; Director of the Center for Cellular Dynamics; Paul Berg Professor of Biochemistry and Molecular Biology
Thesis Supervisor

David Gilmour
Professor of Molecular and Cell Biology
Honors Adviser

* Electronic approvals are on file.

ABSTRACT

Neurons are essential to the structure and function of organisms, making it important to understand the mechanisms underlying their organization and functions. Microtubules are key structural elements of neurons that function as the train tracks of the cell to transport essential cargoes throughout the cell. My research focuses on uncovering the mechanisms that facilitate the localization of γTubulin (γTub) to dendritic branch points where it functions to generate these microtubules throughout the neuron. I hypothesized that the nearby epithelial cells were the source of the initial Wnt ligand that kickstarts the γTub localization pathway. I found that new transgenic lines were necessary to investigate this hypothesis, and I helped in the creation of these lines. I also hypothesized that clathrin-mediated endocytosis was involved in endocytosing Wnts and their receptors to subsequently recruit Wnt signaling proteins to endosomes to propagate the signal. I found that clathrin behaves differently when clathrin-mediated endocytosis is inhibited and after axon injury, with the latter supporting the hypothesis that clathrin-mediated endocytosis may play an upstream role in γTub localization. I also found that levels of disheveled (dsh) were not altered after endocytosis inhibition for a short duration, indicating that a longer inhibition may be needed to generate a significant effect. My findings have further provided the necessary tools and foundations for continued investigation into the mechanisms of the γTub localization pathway at dendritic branch points.

TABLE OF CONTENTS

LIST OF FIGURES

LIST OF TABLES

ACKNOWLEDGEMENTS

I want to thank Dr. Melissa Rolls for her guidance, support, and feedback regarding this project. I also want to thank Alex Weiner for training me at the start of my time in the lab and Pankajam Thyragarajan for further overseeing and assisting with the project. Additionally, I want to thank all the other grad students who worked in the Rolls Lab during my time there who helped support me by providing resources and insight. Finally, I would like to thank my family for their love and support.

This research was funded by the Pennsylvania State University Eberly College of Science and the National Institute of General Medical Sciences.

Chapter 1

Introduction

Drosophila Peripheral Nervous System Organization

The nervous system is crucial to the functioning and survival of an organism as it receives and transmits the signals governing bodily processes and enables the organism to respond to both external and internal environments. One subsystem of the nervous system is the peripheral nervous system, which is responsible for processing and responding to sensory stimuli. Neurons are the cells that make up the basis of this system and are composed of three primary parts. These cells consist of a cell body, which houses the nucleus; a dendrite, which receives the signals and passes them to the cell body; and an axon, which transmits the signals from the cell body to the axon terminal. At this terminal, the axon releases the signal, often in the form of neurotransmitters, into the space between two adjacent neurons. These neurotransmitters then travel to nearby neurons to induce another signal.

Within these neurons, a myriad of components makes neuronal processes and functions possible. Neurons must bring in, or endocytose, various proteins and chemicals that act as signals in pathways, and this process itself involves many key players. These molecules could then go onto aid the neuron's function by initiating signaling cascades, which may produce changes in the organization of cellular components that impact the entire cell's function. To add another level of complexity, cells surrounding the neuron can impact these processes. Understanding the moving parts governing neuronal function is important as it provides greater knowledge of how the human body works and lays the groundwork for medical advancements. However, it is

impossible to study how living human neurons within an intact organism respond to injury or changes in cell expression, which is where model organisms become quite useful.

Drosophila melanogaster is an excellent model organism to investigate the nervous system, partly because of the ease with which its genome can be manipulated for study and the variety of methods available to do so [1]. This manipulation allows for fluorescent tagging of proteins of interest, whose behavior can then be observed via *in vivo* fluorescent microscopy. The translucent nature of *Drosophila* larvae also allows for fluorescent microscopy to be useful in studying the organism's neurons. Finally, the genome of *Drosophila* is very similar to that of the human genome with approximately 75% of the genes responsible for human disease having homologs in *Drosophila* [2].

Within the peripheral nervous system of *Drosophila*, two types of sensory neurons have been identified: type I sensilla and type II multidendritic neurons [3]. Type I neurons use a cilium, and type II neurons have branched dendrites [4]. Dendritic arborization neurons (da neurons) are a type of multidendritic neuron in which the dendrite undergoes extensive branching, therefore forming an arbor [4]. Within *Drosophila* larvae, these da neurons are organized within a series of hemi-segments lining both sides of the larva and extending from its posterior to its anterior end (**Fig 1**). Each hemi-segment contains 15 da neurons, and these da neurons are further subdivided into four classes (I-IV) with Class I being the least branched and Class IV having the most complex branching [3].

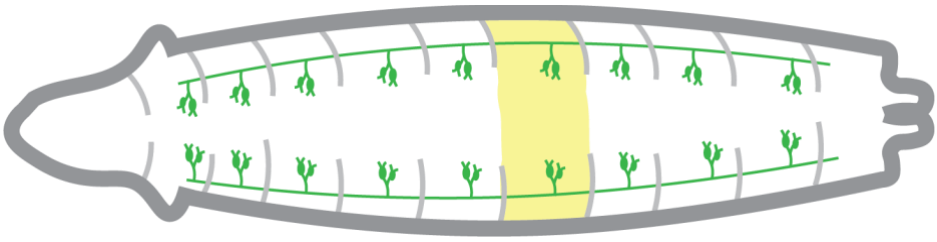

Figure 1: Drosophila neurons are organized within hemi-segments: These hemi-segments span the entirety of the animal from the anterior to the posterior ends, and each hemi-segment contains the same subset of neurons. These neurons can be tagged with green fluorescent proteins, and only Class I neurons are shown for simplicity. One of the regions defined as a hemi-segment is highlighted in yellow. Adapted from Aabha Vora's undergraduate honors thesis.

In my experiments, I study class I neurons due to the simplicity of the primary dendrite and the lack of complex branching. This complex branching is present in higher neuronal classes and often results in confusion as to which dendrite is the primary dendrite [5]. Additionally, in previous studies regarding dendritic branch point nucleation, Class I neurons have been the focus, therefore making them the best class for this study [6], [7]. Within class I, there are three different neurons contained within the dorsal and ventral regions of each hemisegment: ddaD, ddaE, and vpda. These different neurons all contain long dendrites that branch into secondary dendrites. Additionally, the dendrites of neurons in all classes, including class I, do not overlap [5], allowing for clear visualization of neurons and analysis of their properties. The ddaE dendrite is easily identifiable by its comb-like structure and by being the neuron closest to the larval posterior end within each hemisegment. This specific type of neuron acts as an excellent model to study protein localization and uncover the mechanisms making this localization possible.

Neuronal Microtubule Organization

Within neurons, microtubules (MTs) play an essential role in establishing and maintaining neuronal structure and function. Because neurons are cells that stretch far and wide, cargo transport over long distances must occur within neurons to mediate signaling between environmental stimuli and the rest of the body [8]. Motor proteins within families such as the kinesin, dynein, and myosin families accomplish this goal by carrying these cargos along MT lengths [9]. Cargos can include organelles, synaptic vesicle precursors, mRNAs, neurotransmitter receptors, and cell adhesion molecules [9], [10]. MTs are also involved in neuronal migration, initiation, and outgrowth; axonal differentiation, elongation, and regeneration; and synapse formation [8]. Defects in MTs have been associated with diseases including Alzheimer's [11] and Parkinson's diseases, further demonstrating their importance to the functioning of neurons [12], [13]. A crucial property that contributes to these functions is the ability of MTs to grow and shrink rapidly in a process termed dynamic instability [14]

MTs are composed of α- and β-tubulin heterodimers, which associate linearly to form protofilaments, and these protofilaments attach laterally to form a hollow tube (**Fig 2**) [8]. MT growth and shrinkage occur most rapidly at the + end, which ends in the β-tubulin dimer and is regulated by several plus-end tracking proteins [8], [15].

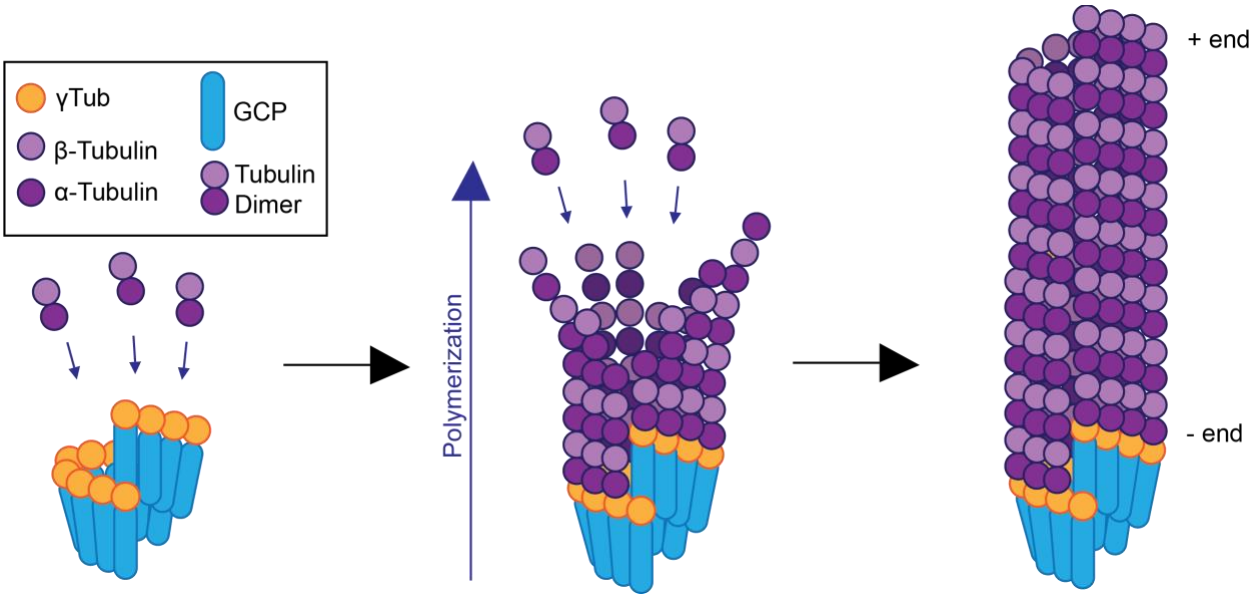

Figure 2: Microtubule structure, polymerization, and polarity: MTs are made of α-β- tubulin heterodimers, and they assemble on a γ-TuRC. The plus end of MTs contains the β-tubulin dimer facing outward and is more dynamic than the minus end. Adapted from Tovey and Conduit, 2018 [16].

In addition to MT dynamics, establishment of MT polarity characterized by which direction the + and subsequent – ends are pointing within the neuron is important in neuronal development. MTs in axons and distal dendrites are plus-end out whereas proximal dendrites contain a mix of minus- and plus-end out MTs [9]. Within *Drosophila* specifically, MT polarity in dendrites changes as the larvae mature with MT polarity being mixed early in development and transitioning to majority minus-end out by the time the larvae are two days old [17] (**Fig 3**). MT polarity is an essential factor in ensuring proper cargo trafficking throughout the neuron given that particular types of motor proteins move specifically towards + ends and others solely towards – ends [9]. But, MTs must first be generated from a point, or nucleated, within the neuron for neuronal morphology and function to be established.

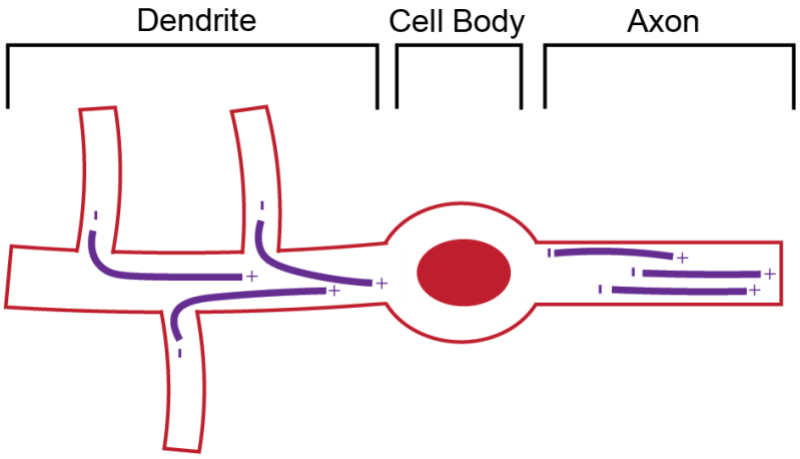

Figure 3: MT polarity differs between axons and dendrites: Within *Drosophila* specifically, MTs in dendrites have minus-ends facing out, or away from the cell body, while axons have plus-ends facing out. MT polarity in dendrites of other organisms is a mixture of plus- and minus-end out.

The γ-tubulin ring complex (γ-TuRC) acts as the MT nucleation site and is made up of proteins of the γ-tubulin complex protein (GCP) family in addition to γ-tubulin (γTub) itself, a homologue of α- and β-tubulin. Within the complex, γTub directly binds the α- and β-tubulin heterodimers, therefore acting as the site from which the microtubule grows (**Fig 2**). The interaction between γTub and heterodimers is especially stable due to the homologies between tubulin subunits [18]. γTub is localized to centrosomes, which are the hub of MT generation and are therefore named the microtubule organizing centers (MTOCs) of the cell [19]. It would make sense for MT generation to occur at the centrosomes because the neuronal cell body contains centrosomes. However, if this were the case, the resulting MTs would be very long. Additionally, γTub is present in neuronal centrosomes during early development, but not after the neurons have formed synaptic connections [20]. In *Drosophila* neurons, the centrioles lack γTub and are not major nucleation sites, indicating that MT nucleation must occur elsewhere [21]. Instead, MT generation occurs at the dendritic branch points in neurons [6].

Dendritic Branch Point Nucleation and Wnt Signaling

At the branch points of dendrites, high levels of γTub are present to engage in this local MT generation [6]. However, γTuRC's alone cannot promote MT nucleation very well and instead must work with other proteins to carry out this function [22]. Some of these proteins include XMAP215, a protein that promotes and accelerates MT growth [23], and CDK5RAP2/centrosomin (cnn), and both of these proteins also function in recruiting additional nucleation machinery to sites in the cell, such as dendritic branch points [24]. But, what signaling pathways are involved in localizing this nucleation machinery, specifically γTub, to these dendritic branch points?

It has been recently found that various proteins involved in canonical Wnt signaling act upstream of γTub and play a role in localizing it to the dendritic branch points [25]. Wnt signaling is a signaling pathway involved in many processes within cells such as cell polarity, proliferation, migration, and fate determination during developmental processes [26]. Canonical Wnt signaling functions through a protein called β-catenin, which is bound by a destruction complex when Wnt signaling is off (**Fig 4A**). This destruction complex consists of APC and Axin bound to GSK3 and CK1. The CK1 and GSK3 function to sequentially phosphorylate the β-catenin, allowing it to be recognized by a ubiquitin ligase and subsequently polyubiquitinated, marking β-catenin for degradation [26], [27]. With β-catenin degraded, gene expression of Wnt target genes does not occur.

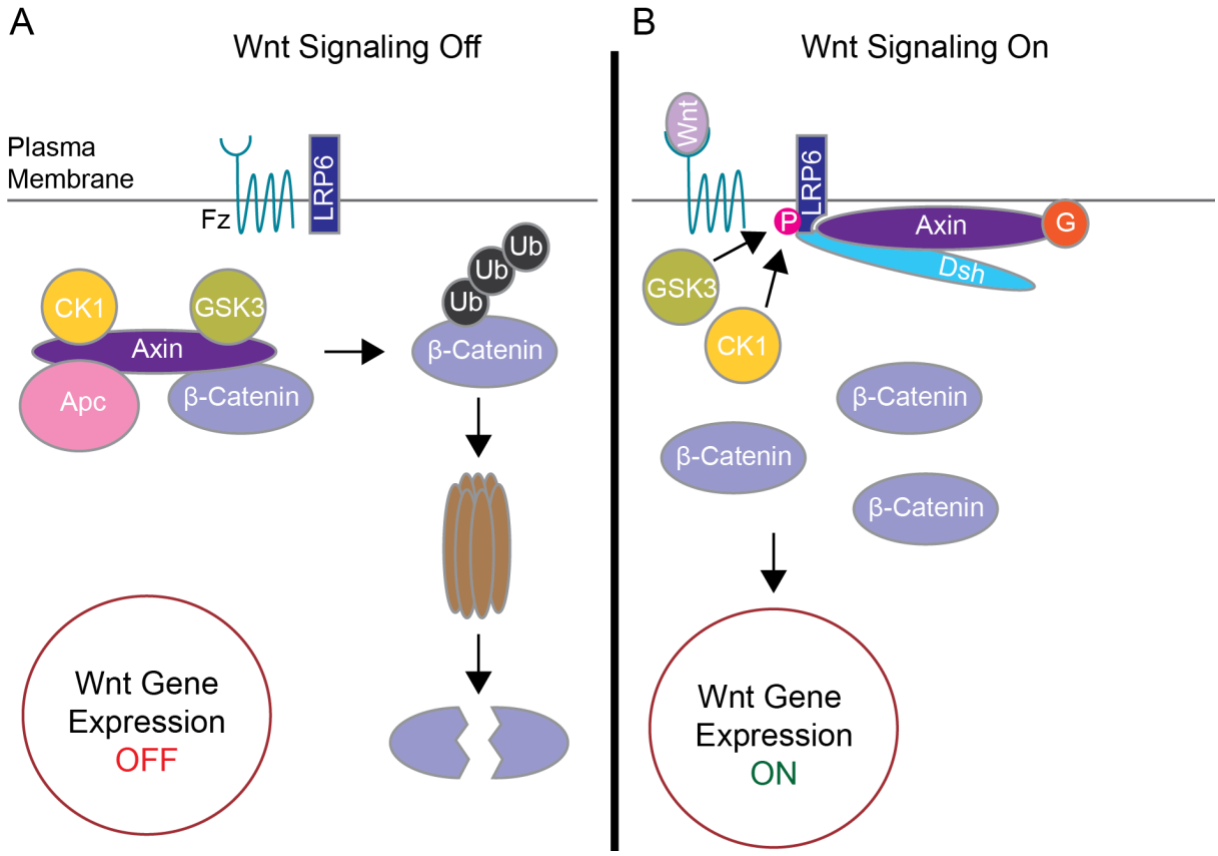

Figure 4: Wnt signaling cascade: When there is no Wnt ligand, β-catenin remains bound to the destruction complex consisting of CK1, GSK3, Axin, and APC. This results in poly-ubiquitination and proteasomal degradation of β-catenin, keeping Wnt gene expression off. When a Wnt ligand binds Fz, LRP6 is phosphorylated to recruit Axin and dsh. This frees β-catenin to enter the nucleus and induce Wnt gene expression. Adapted from Cadigan and Peifer, 2009 [27] and Brunt and Scholpp 2018 [26].

When Wnt signaling is turned on, an entirely different outcome occurs (**Fig 4B**). Canonical Wnt signaling starts with a Wnt ligand binding a receptor, which in this case is Frizzled (Fz) and its coreceptor LRP5/6 [26], [27]. This binding triggers the phosphorylation of LRP5/6's cytoplasmic tail by GSK3 and CK1 [28], which inactivates GSK3 so that it can no longer phosphorylate and target β-catenin for degradation [26], [27]. The phosphorylation of LRP5/6 also creates a binding site for Axin, a scaffold protein in the destruction complex, and this recruitment of Axin disrupts the destruction complex. G proteins, specifically the Galphao subunit, also associate with the Fz receptor and further help to recruit Axin to the plasma

membrane [29], [30]. An additional protein Disheveled (dsh) also localizes to the plasma membrane in response to the Wnt signal where it helps clusters of the Fz/LRP6 receptors oligomerize on the cell surface [27], [31]. In other organisms, Dvl is the abbreviation for dishevelled, but for consistency, the *Drosophila* abbreviation dsh will be used. Dsh also helps with Axin recruitment to the membrane [31]. The result of a nonfunctional destruction complex is that free cytoplasmic β-catenin is not degraded and can enter the nucleus to activate transcription of Wnt target genes [27].

As previously mentioned, Wnt signaling involves the recruitment of various proteins to the plasma membrane, specifically where the Wnt signal has bound to the Fz receptor. However, this protein recruitment is more than a linear progression from one protein to the next and instead involves the formation of a structure called a signalosome. Signalosome formation starts from LRP6 coreceptor oligomerization after Fz binds a Wnt ligand [27]. This focuses the recruitment of subsequent proteins to a distinct location on the plasma membrane and establishes a positive feedback loop where GSK3 phosphorylates LRP5/6, which recruits Axin. Axin in turn recruits even more GSK3, resulting in increased LRP5/6 phosphorylation and the recruitment of more Axin to the membrane [27].

Wnt signaling is important for many cellular processes, one of which includes the localization of MT nucleation sites involving γTub [25]. Several canonical Wnt signaling proteins including fz, fz2, G proteins, Axin, arr, disheveled (dsh in *Drosophila*), and gish have been found to be involved in γTub localization at dendritic branch points as evidenced by reduced γTub concentrations upon RNAi knockdown of these proteins [25]. Additionally, within neurons, it has been found that fz and arr act upstream of dsh, and dsh acts upstream of Axin as in canonical Wnt signaling [25]. Further supporting the involvement of these proteins, Axin

alone can recruit γTub to various cellular sites, and canonical Wnt signaling proteins are needed for normal dendritic MT polarity and for the increase in MT dynamics after axon injury [25], a characteristic injury response in *Drosophila* neurons [32].

Because γTub localization is closely associated with these Wnt signaling membrane proteins, it would make sense for the plasma membrane or an organelle to form the structural basis for these nucleation sites. This is indeed the case as Axin and dsh have been found to colocalize with Rab5 (**Fig 5**) [25], which is a small GTPase at endosomes and is involved in early endocytosis [30]. Moreover, new MT + ends can be generated from puncta marked with fz, dsh, Axin, and Rab5, supporting the idea that Rab5-coated endosomes are a site for MT nucleation [25]. However, we hypothesize that endocytosis must occur in order for these Wnt signaling proteins to be localized to endosomes at dendritic branch points.

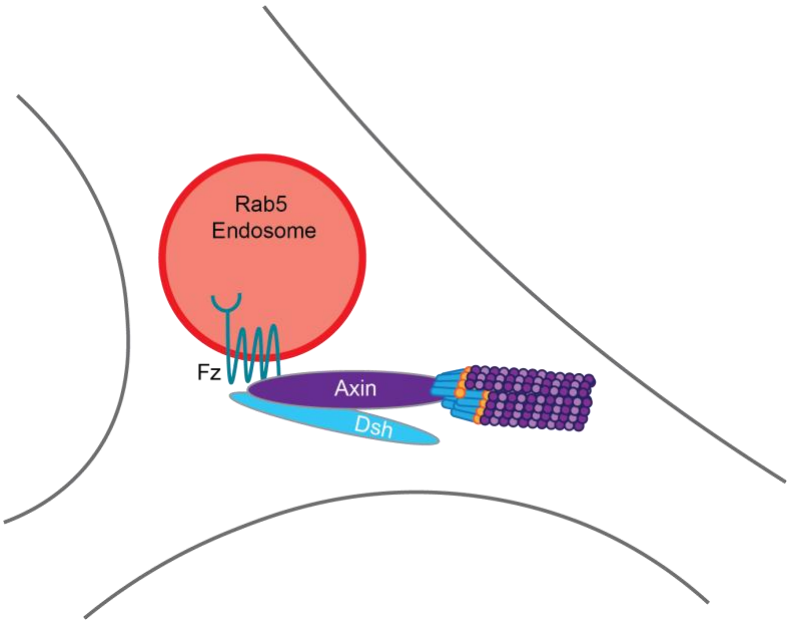

Figure 5: Rab5 endosome at dendritic branch point: Axin and dsh colocalize with Rab5 endosomes, and new MTs can be generated from these endosomes. Adapted from Weiner et al., 2021 [24].

Wnt Signaling and Endocytosis

Endocytosis is the process by which cells bring in extracellular components. At its core, it involves the membrane bending and pinching off to release the vesicle with its cargo into the cell. There are various types of endocytosis, one of which is named clathrin-mediated endocytosis (CME) and involves intracellular proteins called clathrin. Clathrin consists of a heavy and light chain, and three chains of each type assemble to form the clathrin triskelion (**Fig 6A**). In this endocytic process, adaptor proteins such as AP2 bind to the plasma membrane and subsequently recruit scaffold proteins (**Fig 6B**). These scaffold proteins then bind clathrin triskelions, forming a coat on the inner surface of the invaginating membrane. Clathrin facilitates vesicle formation by aiding in membrane bending. Clathrin assembles in an icosahedral cage structure, and because of this rounded shape, the cage encourages the membrane to also adopt a rounded structure. Additionally, actin filaments polymerize at these clathrin-coated sites and interact with clathrin itself to promote membrane invagination [33]. Once the membrane has bent sufficiently, dynamin, a large GTPase, coils around the neck of the forming vesicle and constricts, effectively pinching the vesicle off for full release into the cell. Finally, the endocytic proteins dissociate from the vesicle, freeing it to fuse with endosomes for further intracellular trafficking [33]. The role of endocytosis in Wnt signaling is controversial with evidence supporting claims that endocytosis can promote Wnt signaling and conversely terminate it [34].

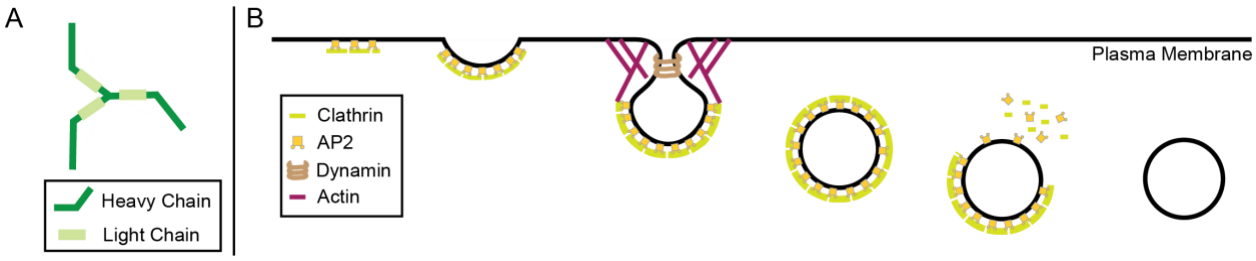

Figure 6: Process of clathrin-mediated endocytosis: A. Clathrin consists of a heavy chain and a light chain, and three of each chain assemble into a structure named the triskelion. Adapted from mechanobio.info [35]. **B.** Clathrin-mediated endocytosis starts with AP2 and subsequently clathrin binding to the plasma membrane. As more proteins are recruited, the membrane bends. Actin later gets involved to help with budding, and dynamin later wraps around the vesicle's neck to pinch the vesicle off into the cell. Membrane uncoating then occurs to free the vesicle to fuse with endosomes in the cell. Adapted from Kaksonen and Roux, 2018 [33].

There is growing evidence supporting that clathrin-mediated endocytosis plays a role in promoting Wnt signaling, and there are several key players involved throughout the endocytic process that impact Wnt signaling [26], [30], [34]. Both clathrin itself and adaptor protein 2 (AP2) are necessary for assembly of the LRP6 signalosomes [36]. AP2 functions in CME by binding both the cell membrane and cargos during the endocytic process, and AP2 is further involved in Wnt signaling due to its μ-subunit binding and stabilizing dsh during endocytosis [33], [37]. Without this AP2-dsh interaction, dsh degrades, the signalosome does not form, and Wnt signaling is decreased [37]. Furthermore, dynamin is necessary for the cell to support high levels of Wnt signaling [38]. Finally, Rab5, which coats endosomes and is associated with Wnt signaling proteins [25], also functions in CME by helping to form clathrin-coated vesicles and fuse these vesicles with early endosomes [30], [39]. Rab5 is also necessary for the cell to support high levels of Wnt signaling [38].

Evidence also exists in support of endocytosis negatively regulating wnt signaling [26], [34]. Endocytosis of Fz receptors can promote their degradation [26]. For example, when Fzd7 interacts with Sorting Nexin27 (SNX27), a protein involved in trafficking cellular cargos [40], it

is endocytosed and subsequently degraded [41]. Additionally, when Fzds are ubiquinated by ZNRF3/RNF43, an E3 ligase, they are endocytosed and undergo proteasomal degradation, which reduces Wnt signaling [34]. Specifically regarding CME, another clathrin adaptor called disabled-2 (Dab2) negatively regulates Wnt signaling by interacting with LRP6 and recruiting it to the CME pathway [26], [42]. This causes a reduction in Wnt signaling because when Dab2 is involved in CME, LRP6 is phosphorylated on S1579 instead of S1490 [42] with S1490 being the phosphorylation site necessary for subsequent Wnt signaling transduction [43]. Overall, the interplay between endocytosis and Wnt signaling is complex, and whether endocytosis promotes or terminates Wnt signaling depends on the presence of specific proteins. Because of this linkage and the involvement of Wnt signaling in MT nucleation, I hypothesize that endocytosis might also play a role in MT nucleation at dendritic branch points within *Drosophila* neurons, potentially by endocytosing Wnts from an external source to further amplify the Wnt signaling cascade involved in localizing MT nucleation proteins.

Because Wnt signaling is involved in the γTub localization pathway [25], it would make sense for a Wnt ligand to also be involved. The neurons are not the source of this initial Wnt ligand, indicating that the initial signal must come from a source outside of the neuron itself [25]. A likely candidate is the nearby epithelial cells.

Interaction Between Skin Cells and Neurons

Within *Drosophila*, the dendrites of dendritic arborization (da) neurons, which are the sensory neurons of focus in this study, branch extensively underneath the epithelia of the larvae, meaning that these neurons are in close proximity to the epithelial cells [4], [5]. Because the

neuron itself is not the source of the initial wnt ligand of the wnt signaling cascade involved in MT nucleation [25], it could originate from a source outside of the cell, and the epithelial cells could be this source due to their proximity to the da neurons. This hypothesis is not unfounded due to evidence that the epithelial cells can interact with and impact neurons.

As the body of any organism continues to grow, the neurons must also grow to continue effectively innervating their area of coverage. During *Drosophila* larval development, the dendrites of class IV da neurons grow very rapidly in the late embryonic and early larval stages, faster than the epithelial cells, and then the rate of dendritic growth slows to match that of the epithelial cells between 48 and 120 hours after the egg has been laid [44]. This phenomenon is referred to as scaling dendrite growth and occurs for the other three classes of da neurons, but at different time points [44]. The epithelial cells were found to play a role in regulating this scaling by producing a microRNA called *bantam*, which performs this function by reducing Akt signaling [44]. Another microRNA called microRNA-9 (miRNA-9) also functions to regulate dendrite growth [45].

MiRNA-9 belongs to a family of microRNAs that regulates neuronal development [46], and in *Drosophila*, the homolog miRNA-9a is expressed only in epithelial cells, not neurons [45]. Another protein involved is a transmembrane receptor named flamingo (fmi) [47], which is also expressed in the epithelial cells, and it functions to promote dendritic growth of class I da neurons when it is expressed at high levels [45]. Within epithelial cells, miRNA-9a functions to decrease fmi expression, resulting in decreased dendritic growth [45]. In this pathway, both the miRNA-9 and the fmi of the epithelial cells perform functions to regulate dendritic growth, further supporting the relationship between epithelial cells and sensory da neurons [45].

Finally, the epithelial cells are involved in the fragmentation and clearing of dendrites during development in *Drosophila* [48]. During larval development, axons and dendrites undergo degeneration and pruning to better establish the neural connections required for function in adulthood [49], [50]. The resulting debris must be cleared for the successful growth of new neurons [51] and to prevent neuroinflammation, which can cause neurodegenerative disease if left unregulated [52]. The epithelial cells function to phagocytose and clear this dendrite debris, and they also facilitate dendritic fragmentation in pruning and dendrite injury by extending membrane regions rich in actin to wrap the dendrite branches [48].

In this thesis, my overall goal is to determine the mechanisms that act upstream of γTub localization to the dendritic branch points. Specifically, my focus is on the source of the initial Wnt ligand and how this ligand and its receptors might enter the neuron to kickstart the Wnt signaling cascade involved in γTub localization (**Fig 7**).

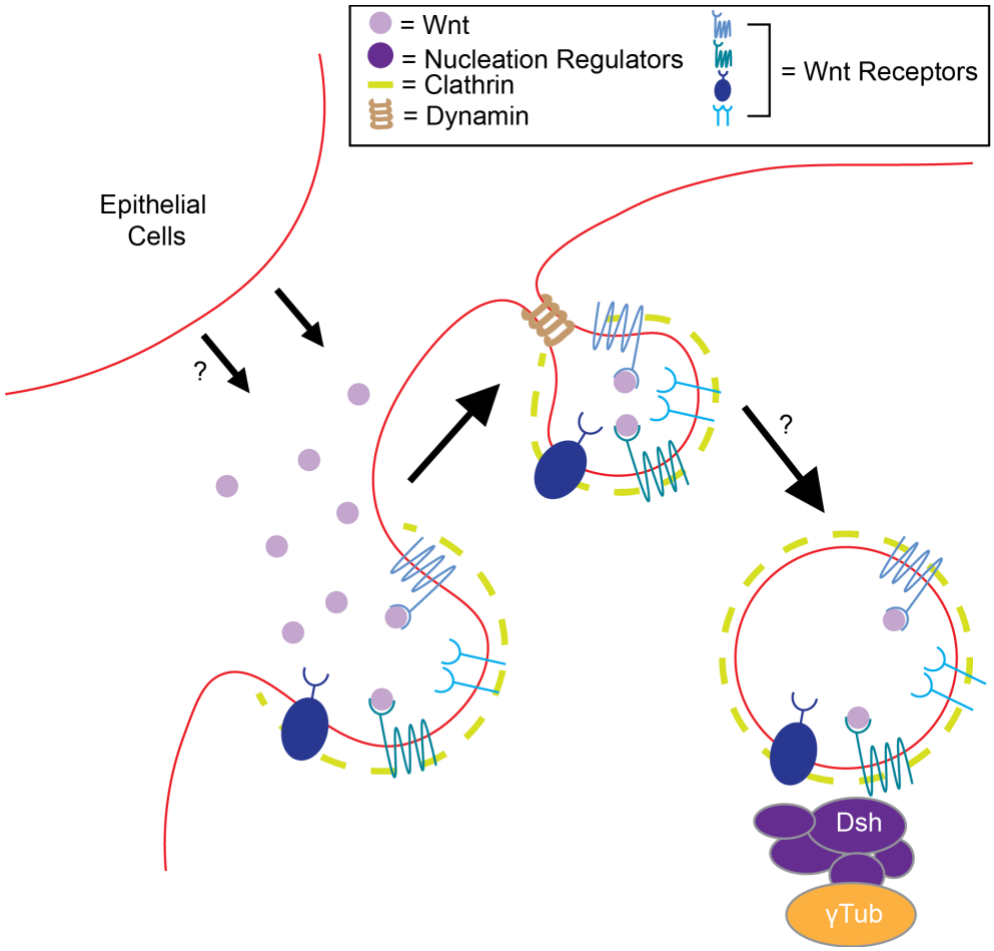

Figure 7: Proposed mechanism for wnt ligand secretion and endocytosis in the γTub localization pathway. We hypothesize that the epithelial cells are the source of the initial wnt ligands of the γTub localization pathway and that these ligands and their receptors are endocytosed via clathrin-mediated endocytosis to further transmit the signal inside of the neuron.

Chapter 2

Results

A Tester Line Containing the Gal4 System Alone Cannot Be Used to Investigate Epithelial Wnt Function

In microtubule nucleation at dendritic branch points, γ-tubulin localizes to dendritic branch points and is essential for the initiation and growth of microtubules at these branch points [6]. Additionally, Wnt signaling plays a large role in recruiting γTub to the branch points. Neurons themselves produce Wnts, but these specific Wnts do not impact γTub localization [25], leading us to investigate extracellular sources for this ligand. The sensory da neurons of this study are in close proximity to the epithelial cells [4], and epithelial cells and neurons interact in a variety of processes to accomplish specific tasks within the animal [53], [54]. **This leads us to hypothesize that the epithelial cells may be the source of the initial Wnt signals responsible for initiating the signaling cascade responsible for γTub localization**. To investigate this hypothesis, I aim to perturb Wnt secretion in epithelial cells and observe the impact this has on γTub localization at dendritic branch points.

The first step in this investigation involved constructing a skin cell tester line (**Fig 8**) to use in conjunction with various RNAi lines to effectively inhibit wnt secretion from the epithelial cells (**Fig 9**). I took Z stack images of larvae within each cross and quantified the fluorescence intensity of γtub at each branch point. Each cross consisted of an RNAi crossed with a skin cell tester line (UAS-mCD8-RFP; UAS-γTub-GFP, A58-Gal4). This tester line expresses the membrane marker mCD8-RFP and γTub-GFP in the epithelial cells using the A58 driver. The intention was to have 221-Gal4 included in this line to express both mCD8-RFP and γTub-GFP

in the class I neurons as well, however, some issues in screening resulted in selecting larvae expressing these proteins in a different subset of neurons. Despite this, we chose to use this line for experimentation because we thought it would still provide useful data.

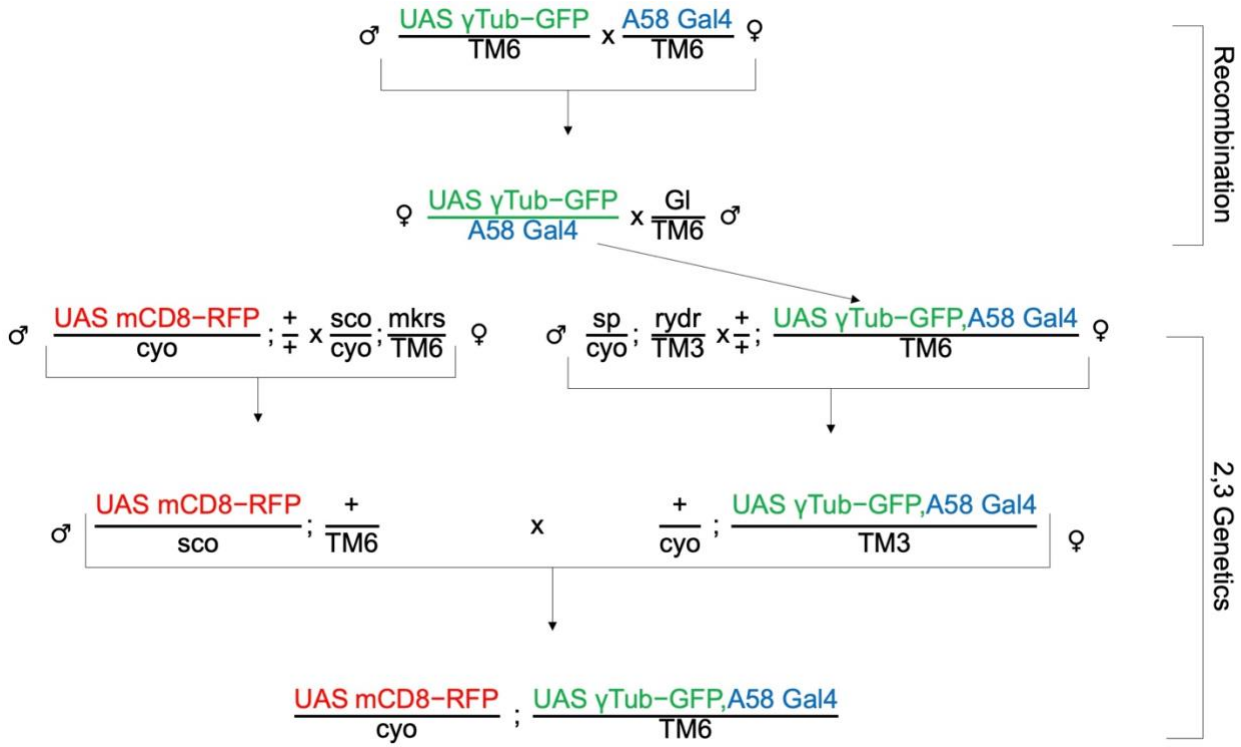

Figure 8: Mating scheme to create skin cell tester line: Creating this line involved several crosses. The first set of crosses involved recombination and screening of larvae to ensure the correct genotype, and the second set of crosses involved 2,3 genetics to get desired genes from different chromosomes into the same line.

Within this set of experiments, I used several RNAi's targeting specific genes. Rtnl2 RNAi served as my control since the presence nor the absence of this protein presents a phenotype, and two different wntless lines (abbreviated Evi 46/47) served as my experimental conditions. In *Drosophila*, wntless is a transmembrane protein responsible for regulating Wnt secretion [55], so knocking down this protein effectively inhibits wnt secretion of the epithelial cells, allowing me to investigate the impact this may have on γTub levels at the dendritic branch points.

However, due to the extensive expression of γTub in the epithelial cells, there was too much background expression to reliably determine the level of γTub at the branch points, resulting in inconclusive data (**Fig 9**). I tried to subtract out the background levels near each branch point to minimize the effects of this interference, but the results were inconclusive. Therefore, a new skin cell tester line is needed to continue in these experiments.

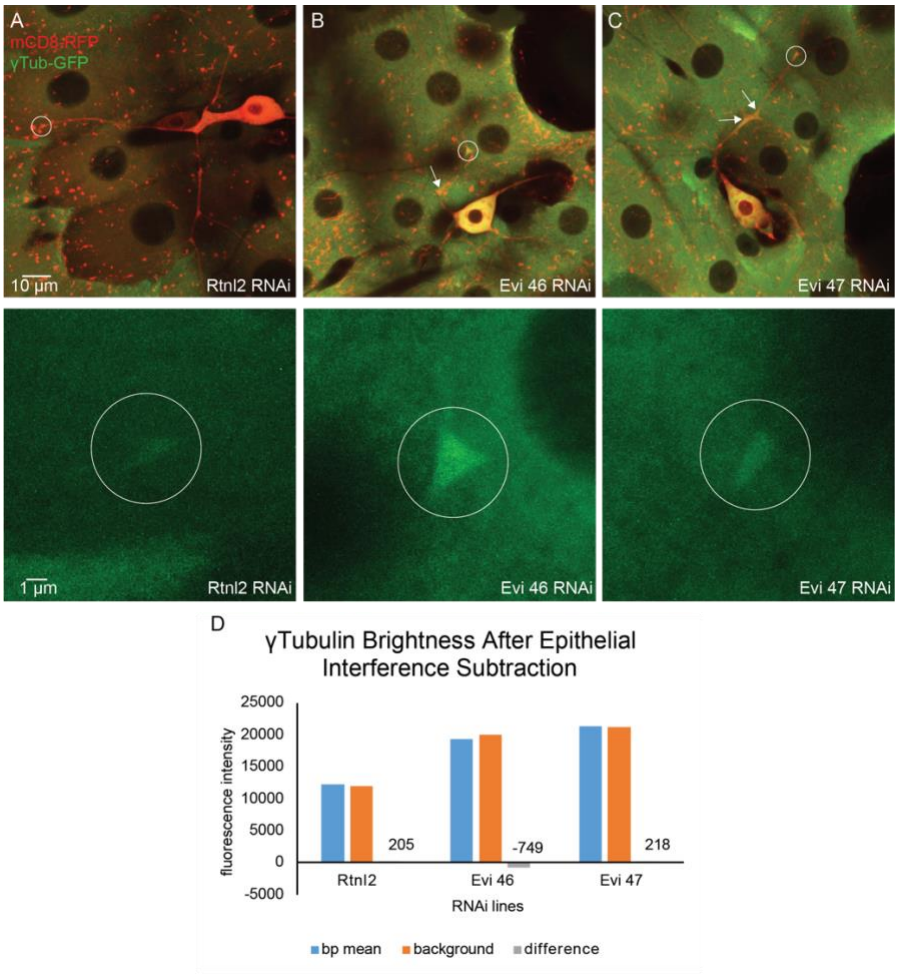

Figure 9: A new skin cell tester line is needed to determine the effect of inhibiting epithelial Wnt secretion on γTub localization: Neurons are clearly visible in A-C, however the significant amount of background expression in the epithelial cells prevented accurate quantification of γTub intensities at branch points. Subtracting the fluorescence intensity in the epithelial cells at points near each branch point did not allow for production of reliable results, further indicating the need for a new skin cell tester line. Arrows and circles indicate branch points of interest with each circle indicating the zoomed image of the branch point below its corresponding image.

A Q-System Tester Line Effectively Separates Epithelial and Neuronal Expression

Because background epithelial interference is an issue in the current skin cell tester line, it is essential that the new skin cell tester line eliminates this issue. To address this, the new skin cell tester line will involve two transcription systems to ensure that certain genes are expressed exclusively in the epithelial cells while other genes are exclusively expressed in the neurons. The first of these transcription systems is the Gal4/UAS system, which involves the binding of the gal4 transcription factor to an upstream activating sequence (UAS) that is upstream of target genes [56]. The second of these systems is the Q system, which functions similarly but instead involves a QF transcription factor binding to an upstream QUAS [57]. Furthermore, each of these transcription systems will be targeted to specific cell subtypes by attaching the transcription factor genes to tissue- or cell-specific drivers [58]. In this context, the gal4 transcription factor will be expressed only in the epithelial cells under the epithelial cell driver A58 while the QF transcription factor will be expressed only in the class I dendritic arborization (da) neurons under the TMC driver (**Fig 10**). The result of this is that the epithelial cells will express the RNAi that is targeting Wnt secretion, and the class I da neurons will express γTub-GFP and mCD8-RFP, eliminating the background epithelial γTub-GFP expression.

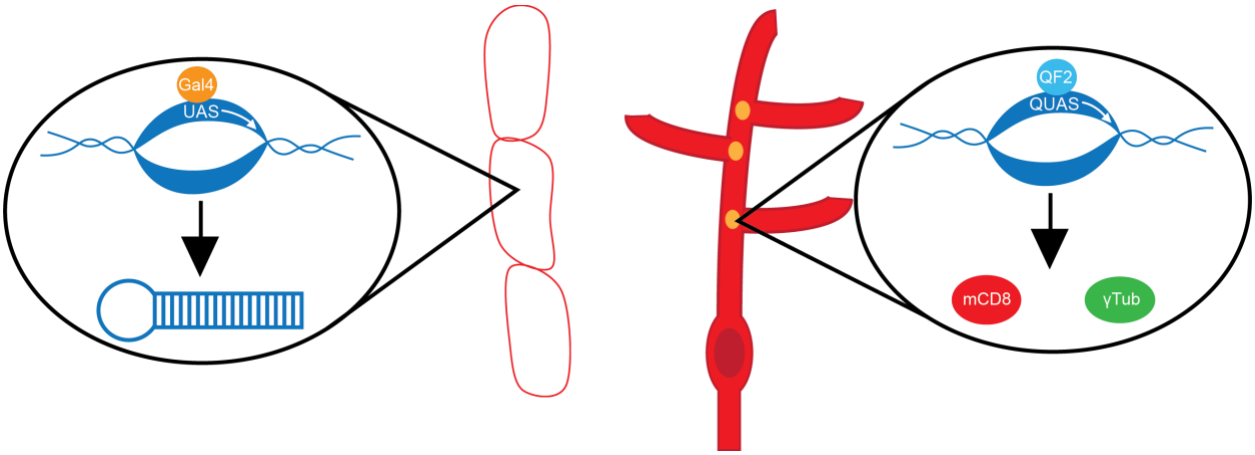

Figure 10: The GAL4/UAS system will function in the epithelial cells while the QF2/QUAS system will function in the class I da neurons. The result of this is that expression of the RNAi will be restricted to the epithelial cells and the expression of the mCD8-RFP and γTub-GFP will be restricted to the class I da neurons. This will eliminate the interfering γTub expression in the epithelial cells because they will not express the necessary transcription for mCD8 and γTub expression.

At the time I was working on this line (spring 2020), our lab did not have any vectors containing a QUAS-γTub-GFP, so I aided our lab tech in converting the UAS of the UAS-γTub-GFP construct into a QUAS for insertion into the final line. The expansion of the COVID-19 pandemic interrupted my work on this project. However, since then, this new line has been completed and with all of its components is as follows: QUAS-γTub-GFP, QUAS-myr-tdtomato, TMC-QF/Cyo; A58-gal4, dicer2-nLS-BFP/TM6 (**Fig 11**). We can ensure that all of the fluorescently tagged components are in the line since they are visible via fluorescence microscopy. In the specific cross in **Fig 11**, the new tester line was crossed with UAS-mCD8-GFP to ensure that the skin cell driver was in the cell. For the drivers (ie TMC-QF, A58-gal4), which do not not exhibit fluorescence, we know they are in the line because without them, neuron-specific expression of both γTub-GFP and myr-tdtomato and epithelial-specific expression of mCD8-GFP in this particular cross would not be possible. Future xperiments with

this line will not involve epithelial expression of GFP but will instead involve expression of RNAi's to knock down specific wnts.

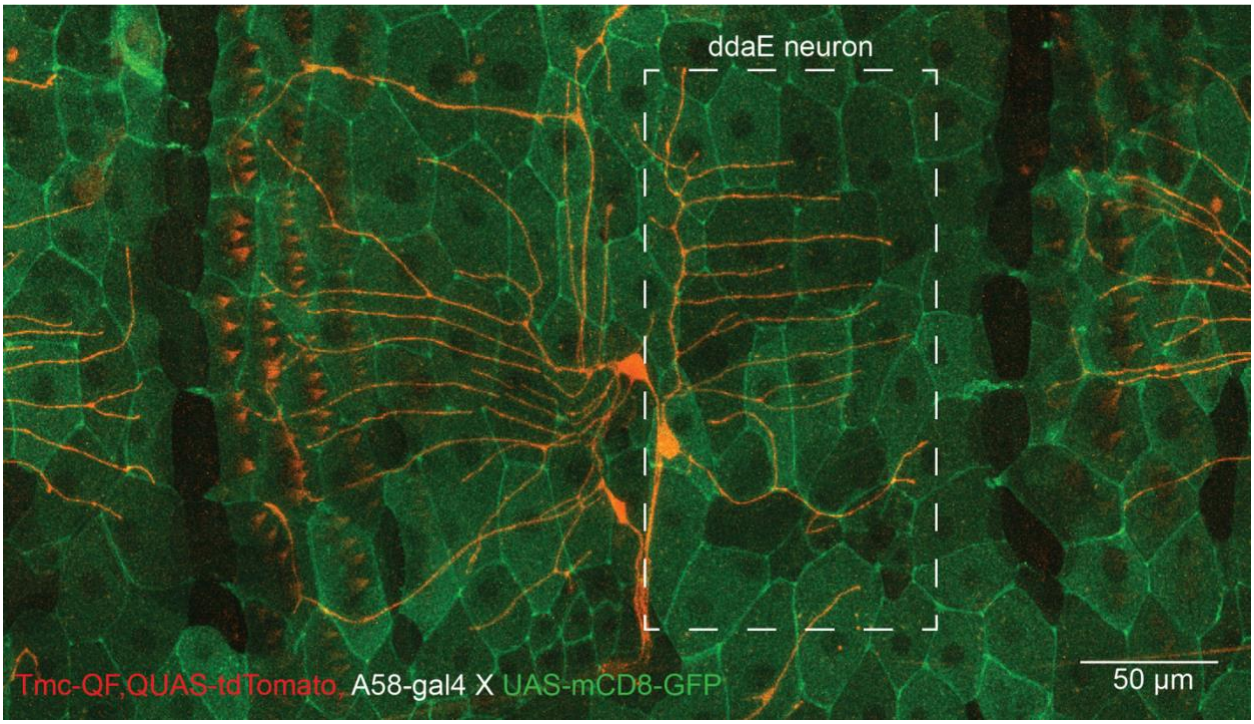

Figure 11: New skin cell tester line: This completed skin cell tester line using both the QUAS and UAS transcription systems to separately regulate gene expression in the epithelial cells and the neurons. The white box indicates the ddaE neuron, which is the neuron of focus in these investigations, with its characteristic comb dendrite. Image and figure format from Pankajam Thyagarajan.

Because of the amount of time required to create this essential line, I shifted the focus of my project to another aspect of the γTub localization pathway: how the initial Wnt ligands enter the neuron. Because of the involvement of clathrin-mediated endocytosis in Wnt signaling [26] and the presence of clathrin at the dendritic branch points, I shifted my focus to investigating the role that clathrin-mediated endocytosis might play in γTub localization.

Inhibiting Clathrin-Mediated Endocytosis Induces Measurable Changes in Clathrin Present at Dendritic Branch Points

Clathrin-mediated endocytosis is a mechanism by which the cell brings in materials from the outside. In this process, clathrin forms a cage-like structure around the vesicle as it is budding into the cell, and a protein called dynamin constricts around the neck of the budding vesicle to pinch the membrane and release the vesicle fully in the cell where it can fuse with endosomes. Various Wnt signaling proteins involved in γTub localization localize on Rab5 coated endosomes at dendritic branch points, and growth of new MTs can be initiated from these endosomes [25]. For these reasons, **we hypothesize that clathrin-mediated endocytosis is the mechanism by which these Wnt signaling proteins arrive to Rab5 endosomes to facilitate γTub localization at dendritic branch points.**

Before conducting experiments to determine how the inhibition of endocytosis affects proteins involved in the γTub localization pathway, we decided to first characterize the behavior of clathrin itself at dendritic branch points by observing its behavior when clathrin-mediated endocytosis was inhibited. This experiment consisted of one cross involving a line containing clathrin tagged with GFP (UAS-EGFP Clc on II) and a shibire mutant line (shi^{ts1}), which functions to inhibit clathrin-mediated endocytosis. Shibire itself is the *Drosophila* homolog for dynamin [59], which constricts to pinch off clathrin-coated vesicles into the cell [33]. Shi^{ts1} contains a mutation on the X chromosome [60], and the temperature-sensitive nature of this mutant means that in order for the mutation to become activated, the animal must be exposed to high temperatures, specifically 29 °C in this case [61]. This is convenient because I can then activate the mutation by incubating larvae immediately prior to imaging. The mutation specifically inhibits dynamin from exhibiting its constriction function at high temperatures,

which prevents vesicles from being fully released into the cell. The vesicles are instead arrested at the cell membrane [62]. Additionally, because this mutation is on the X chromosome [60], only males will express the mutation, meaning that there needs to be a way to separate male larvae from female larvae for experimentation.

When larvae expressing the mutation (males) are exposed to high temperatures, they also exhibit a paralysis phenotype [61], whereas those without the mutation (heterozygous females) retain their movement abilities. Additionally, when male larvae are compressed under a microscope slide, their gonads are visible as two translucent circles towards the animal's tail (see **Fig 15** in methods section), adding an additional measure to ensure that paralyzed larvae are indeed males.

To make imaging more efficient, I screened larvae prior to imaging to isolate mutant (male) larvae. I did this by incubating larvae for 15 minutes, isolating the paralyzed larvae, and letting them recover for between two and twelve hours. After that time, I incubated larvae for 15 minutes immediately prior to imaging to induce the heat shock again. After this second heat shock, I made sure that the mutant larvae exhibited both the paralysis phenotype and visible gonads, and I considered larvae that lacked gonads but retained movement as wildtype, with wildtype referring to the heterozygous females that do not express the mutation. The data I collected for this experiment was in the form of videos approximately five minutes in length in addition to a couple of overview images.

At the branch points of the class I ddaE dendrite, clathrin was visible as puncta of varying sizes (**Fig 12A**). Within the videos, I noticed that there were puncta within the branch point that remained stationary and others that visibly cycled within the branch point (**Fig 12B**). In quantifying the differences between in the percentage of branch points containing mobile clathrin

puncta, a significantly smaller proportion of branch points within mutants contained mobile puncta (**Fig 12C**). Although this increase was slight, I know it is attributed to the successful induction of the shibire mutation because the mutation is induced at 29°C [61], and my experimental conditions include incubation at 37°C, which is above this incubation threshold. Additionally, clathrin-coated vesicles were arrested at the cell surface after a 5- or 10-minute incubation at 30°C [62], making my incubation time of 15 minutes sufficient to arrest endocytosis. Finally, there was no difference in the number of stationary puncta between the wildtype and mutant conditions (**Fig 12D**).

In addition to characterizing clathrin using the genetic backgrounds described above, I also noticed that the gonads exhibited green fluorescence due to the line expressing clathrin tagged with GFP. The ability to identify the gonads using fluorescence microscopy proved to be helpful in situations where it was not clear if gonads were present.

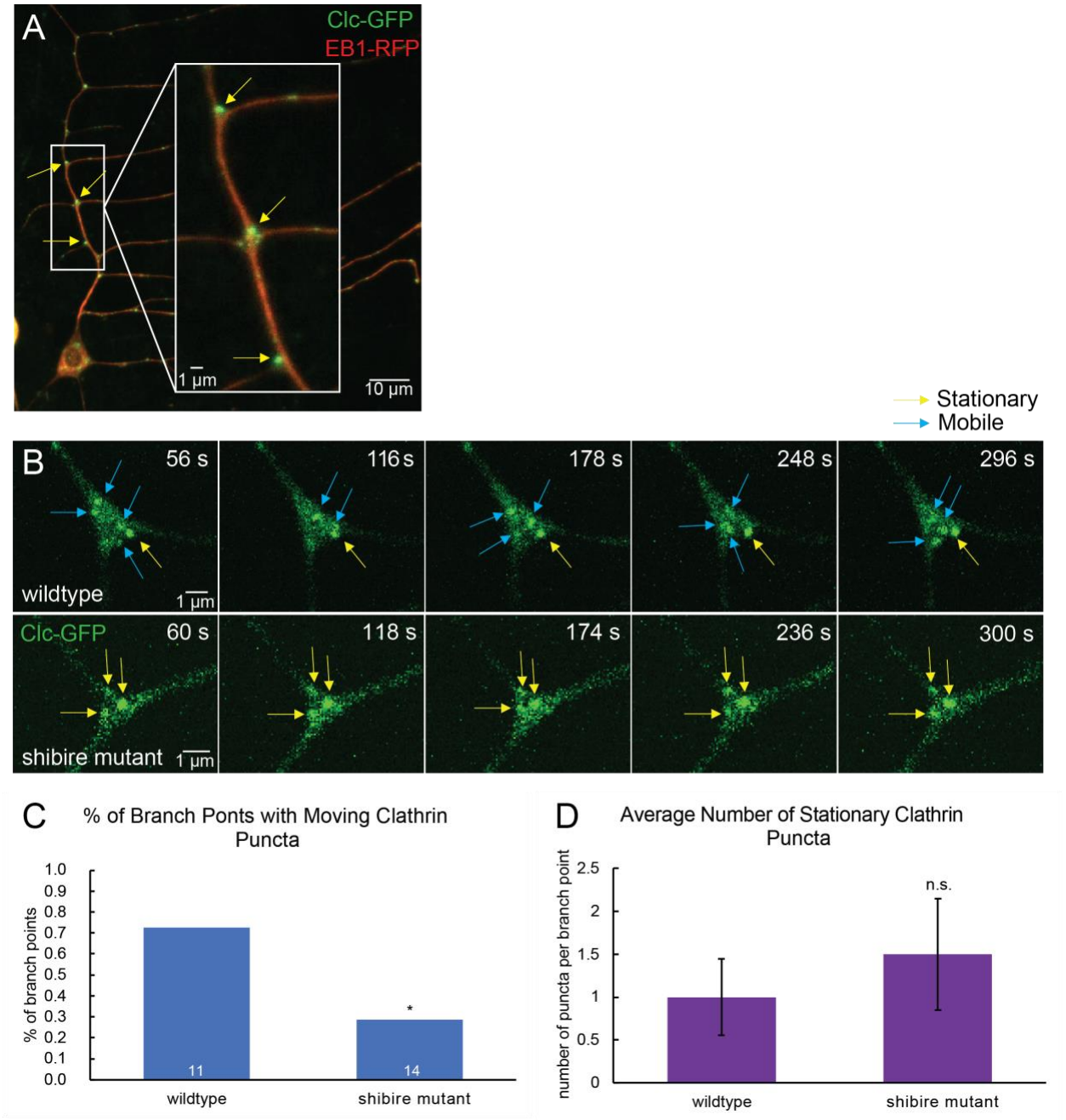

Figure 12: Inhibition of clathrin-mediated endocytosis decreases the mobility of clathrin puncta in shibire mutants but does not affect the number of stationary puncta per branch point: Clathrin gather in puncta at dendritic branch points, and these puncta either remain stationary or visibly move within the branch point. A smaller percentage of branch points contained moving clathrin puncta when endocytosis was disrupted, but the number of stationary puncta was not different per branch point was not different. Error bars indicate standard deviation, and n refers to the number of branch points examined.

Inhibiting Clathrin-Mediated Endocytosis for 15 Minutes Prior to Imaging Does Not Affect the Amount of Disheveled at Dendritic Branch Points

Dsh is a Wnt signaling protein that localizes to the plasma membrane and cytosol and helps with oligomerization of Wnt receptor complex of Fz and LRP6 on the cell membrane and with recruitment of Axin to this forming oligomer [27], [31]. Additionally, dsh interacts with the μ2 subunit of AP2, an adaptor protein involved in CME [33], and this interaction stabilizes dsh and allows for successful internalization of the signalosome [37]. Dsh (disheveled in *Drosophila*) is also one of the upstream Wnt signaling proteins involved in γTub localization and subsequent MT nucleation at dendritic branch points [25]. Because of this evidence and the localization of both clathrin and dsh at the dendritic branch points, **we hypothesize that inhibiting clathrin-mediated endocytosis will decrease the amount of dsh present at the branch points, thereby affecting MT nucleation.**

In order to test this hypothesis, I used the shibire^{ts1} mutant crossed with a dsh tester line (UAS-mCD8-RFP/CyO; 221-Gal4, UAS-dsh-GFP/TM6) as my experimental group and yw crossed with the same dsh tester line as my control group. This tester line functions to express both a membrane marker (mCD8-RFP) and dsh (dsh-GFP) specifically in class I da neurons. For both groups, I incubated 3rd instar larvae for 15 minutes to isolate paralyzed shibire mutants and let them recover for between two and twelve hours. After that time, I incubated larvae for 15 minutes immediately prior to imaging to induce the heat shock again. I considered larvae with visible gonads and the paralysis phenotype as mutants. The data I collected for this experiment was in the form of overview images of the class I ddaE neuron (**Fig 13A-B**) and zoomed images of the dendritic branch points of the comb dendrite of this same neuron subtype (**Fig 13C-D**).

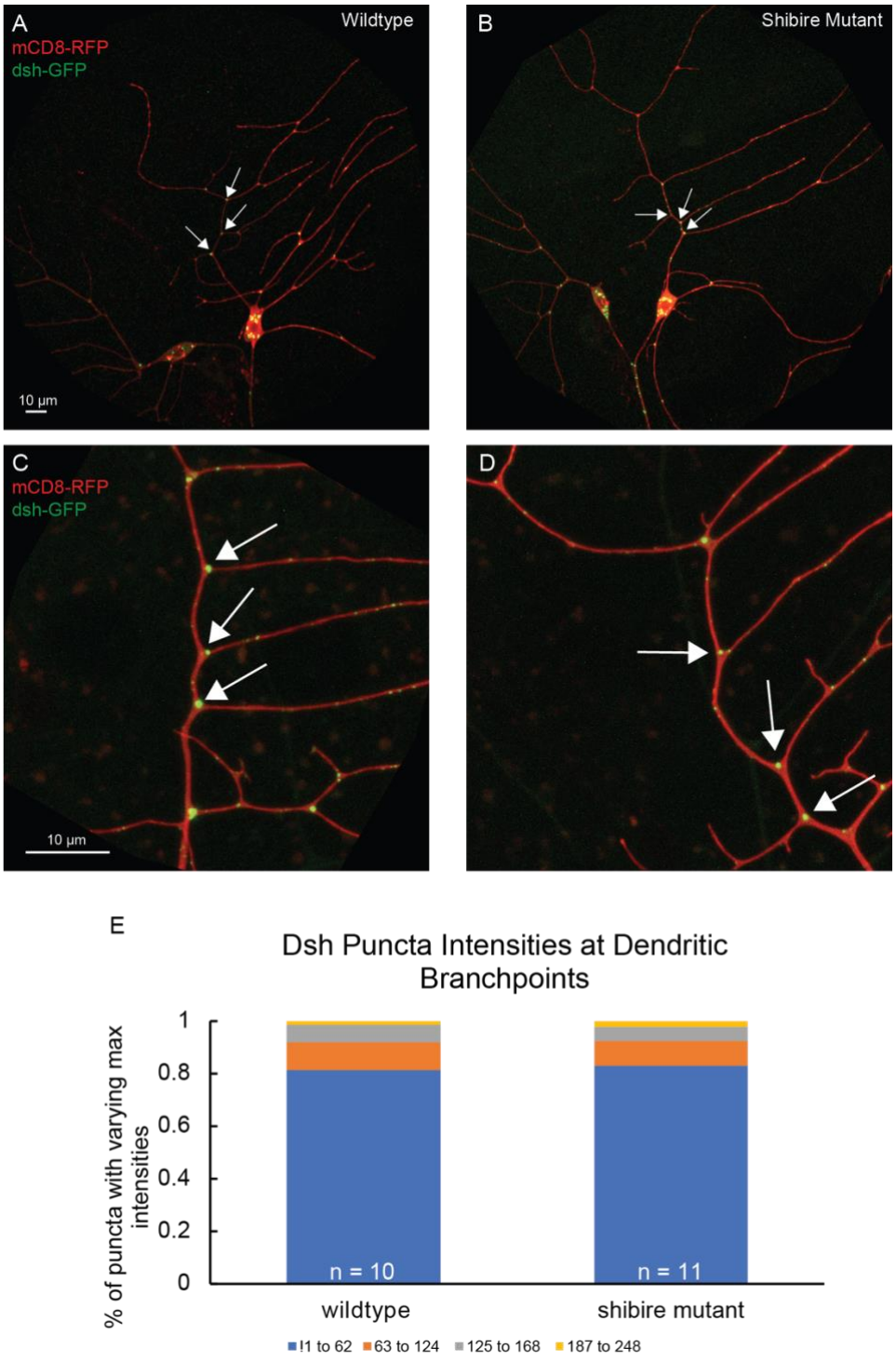

Figure 13: Dsh localization in dendritic branch points is not different after inhibition of clathrin-mediated endocytosis: Both the wildtype and shibire mutant larvae have dsh puncta of varying intensities at the dendritic branch points, but there is no difference between the distribution of fluorescence intensities.

Dsh formed puncta at the dendritic branch points in both the wildype and mutant larvae, and the puncta at these branch points varied in intensity with both groups having puncta that were very bright and others that were quite dim. After determining the maximum fluorescence intensity of each punctum, values within wildtype and mutant groups were assigned to categories of intensity ranges to assess the distribution of puncta intensity. From this analysis, there does not appear to be a difference in the amount of dsh present at the dendritic branch points between the wildtype and mutant groups (**Fig 13E**). This could be because CME may not have been inhibited long enough to generate a phenotype, and as a result, additional experiments involving a longer heat shock are in progress to continue determining the effect that CME has on Wnt signaling and subsequent MT nucleation within *Drosophila* sensory neurons.

Clathrin Behaves Differently 8h After Axon Injury

After axon injury, one way the neuron responds is by increasing MT dynamics, as evidenced by an increase in EB1 comets after axon injury [7]. This upregulation of MT dynamics relies on an increase in MT nucleation, facilitated through the action of γTub [32]. Because of this increase in MT nucleation after axon injury, **we hypothesize that if clathrin-mediated endocytosis does play a role in MT nucleation and subsequent γTub localization, clathrin activity should also be upregulated after axon injury.**

In order to test this hypothesis, the larvae imaged expressed Clc-GFP and EB1-RFP, with EB1-RFP providing an indicator of EB1 dynamics in the case that axon injury was not clear at 8h. Both larvae that did and did not undergo axon injury were imaged, with 0h representing the uninjured group and 8h representing the injured group. Axon injury was conducted using a UV

pulse laser, and the injured neuron was imaged 8h after injury. The data collected for this experiment involved overview images of the ddaE neuron within the 8h group to ensure that axon injury had occurred (**Fig 14A**) as well as 5-minute videos focused on dendritic branch points within the comb dendrite of those ddaE neurons (**Fig 14B**).

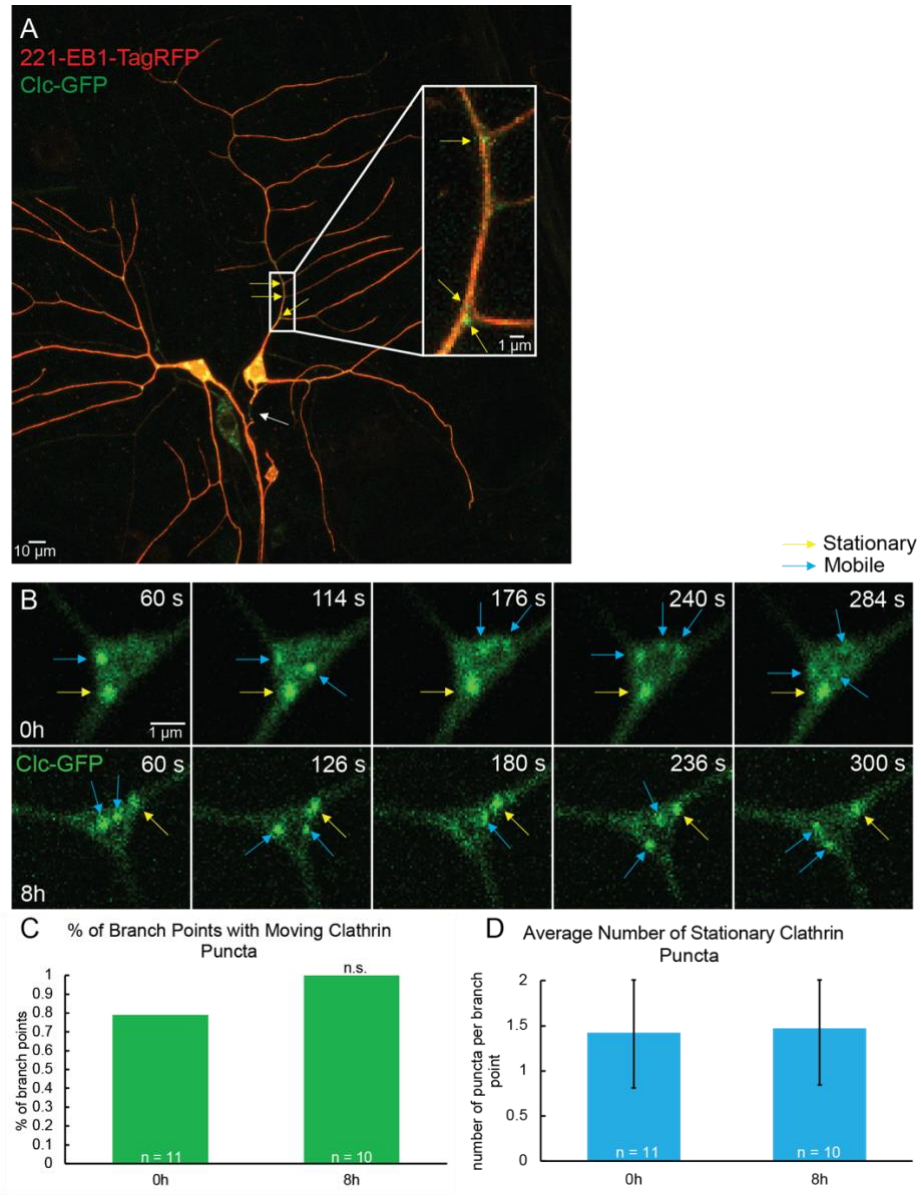

Figure 14: Axon injury does not affect the average number of stationary clathrin puncta but does slightly increase clathrin puncta mobility: In the overview image, the white arrow indicates the site of axon injury 8h after injury, and the yellow arrows indicate branch points containing clathrin puncta. Both 0h (uninjured) and 8h (injured) dendritic branch points have

mobile and stationary clathrin puncta. There appears to be a slight increase in clathrin mobility after injury but no difference between the average number of stationary clathrin puncta. An increased sample size is necessary to determine if this effect is significant. The abbreviation n.s. indicates no significance of results, and error bars indicate standard deviation. Sample sizes indicated refer to the number of animals assayed.

Similarly to clathrin behavior in the assay involving CME disruption, both clathrin mobility and the number of stationary clathrin puncta were assessed in the presence and absence of axon injury. There were no changes in the average number of stationary puncta at each branch point (**Fig 14D**), however, there was a slight increase in clathrin mobility after axon injury (**Fig 14C**). However, this increase was not statistically significant. Due to the small sample size, it is possible that this increase will be more pronounced and potentially significant with an increased sample size, which will allow for a more definitive conclusion to be drawn about the role of clathrin-mediated endocytosis in MT nucleation. Regardless, this preliminary data does indicate an upregulation in CME after axon injury, which does not dismiss the possibility of CME involvement upstream of MT nucleation.

Chapter 3

Materials and Methods

Drosophila Stocks and Genetics

All *Drosophila* stocks were obtained from Indiana University's Bloomington *Drosophila* Stock Center as well as from the Vienna *Drosophila* Resource Center (VDRC). All RNAi, mutant, and tester lines used in these experiments are included in the tables at the end of this section (**Tables 1** and **2**).

These fly lines were grown and maintained in a plastic bottle with fly media at the bottom, and all bottles were plugged with cotton plugs. The flies were flipped into new bottles about every 2-4 weeks to prevent the proliferation of mites and microbes. All fly lines were stored at 25°C with the exception of shibire^{ts1}, which was stored at 20°C due to the temperature sensitive mutation.

In order to perform experiments using these lines, various crosses were set up with selected males and females. All crosses involved the selection of virgin females because after mating, females retain sperm from males they have previously mated with and continue using that sperm to fertilize subsequent eggs. Selecting virgin females guarantees that the females are storing no sperm from previous mating, ensuring that the cross remains uncontaminated. Virgin flies are unique in that they have a dark spot on their abdomens and are therefore easily identifiable. Virgins were also selected if it was known that they were less than 8 hours old. These virgin females were mated with males with specific physical markers indicating their possession of desired genes.

The tester lines utilized in these experiments are as follows: (UAS-mCD8-RFP; UAS-γTub-GFP, A58-Gal4), (UAS-Dcr2, UAS-mCD8-RFP; 221-Gal4, UAS-γTub-GFP), (UAS-clc on 2; 221-gal4, UAS-EB1TagRFP-T/TM6), (UAS-mCD8-RFP/CyO; 221-Gal4, UAS-dsh-GFP/TM6), and (dicer2, mCD8-RFP/CyO; 221-Gal4, γTub GFP/TM6).

Table 1: *Drosophila* RNAi and Mutant Lines

Name	**Abbreviation**	**Chromosome**	**VDRC/Bloomington #**
Reticulon 2	Rtnl2	2	V33320
Wntless (A15346)	Evi	3	V5214
Wntless (A15347)	Evi	3	V5215
Shibire^{ts1}	Shi^{ts1}	X	BL7068

Table 2: Other Transgenic *Drosophila* Lines

Name	Experiment
UAS-mCD8-RFP; UAS-γTub-GFP, A58-Gal4	γTub localization tester line
UAS-Dcr2, UAS-mCD8-RFP; 221-Gal4, UAS-γTub-GFP	γTub localization
Dicer2, mCD8-RFP	Determining best skin cell driver
w;;A58-gal4/TM6B	Skin cell driver
w;e22c-gal4 (II)	Skin cell driver
Gl/TM6	Balancer (skin cell tester line construction)
sp/cyo; rydr/TM37	Balancer (skin cell tester line construction)
sco/cyo; mrks/TM6	Balancer (skin cell tester line construction)
UAS-Dcr2, UAS-mCD8-RFP on II	Skin cell tester line construction
UAS-EGFP Clc on II	Clathrin localization
221-gal4, UAS-EB1TagRFP-T/TM6	Clathrin localization post axotomy
yw	dsh localization
UAS-mCD8-RFP/CyO; 221-Gal4, UAS-dsh-GFP/TM6	dsh localization

Plasmid and Tester Line Construction

A new skin cell tester line was constructed that utilizes the Gal4 system for expression in epithelial cells and the Q system for expression in neurons with genotype QUAS-γTub-GFP, QUAS-myr-tdtomato, TMC-QF/Cyo; A58-gal4, dicer2-nLS-BFP/TM6. Molecular cloning was used to convert the UAS- γTub to QUAS- γTub for successful binding of the QF2 transcription factor.

To convert the UAS to QUAS, the 5x UAS and hsp70 promoter sequences were removed from the γTub-GFP vector with SphI and BglII. This fragment was gel isolated and cloned into

the 2771 bp fragment of the 1GCT pHD-dsRed plasmid, also cut with SphI and BglII and gel isolated. 1GCT and 5x-UAS-hsp-promoter fragments were transformed into *E. coli* and sequenced to ensure success.

Two strategies were implemented for Q5 Site-Directed Mutagenesis to insert QUAS and delete the 5x UAS. The goal of the first strategy is to clone in a 4x QUAS. The PacI site was introduced via Q5 Site-Directed Mutagenesis using two unique primers and Herculase:

Q5 PacI forward primer: TTAACGGAGACTCTAGCGAGCGCCGGAGTATAAATAG

Q5 PacI reverse primer: TTAAACCTGCAGGCATGCGAATTCCACCTGCTTCAG

The 4x QUAS was removed from the QFT QUAS E1B NLS Cardinal construct using PacI, gel isolated, and cloned into the 1GCT backbone to give a 4x QUAS construct.

The goal of the second strategy is to clone in an 8x QUAS. The blunt sites ZraI were introduced in addition to the deletion of the 5x UAS using Q5 Site-Directed Mutagenesis with two unique primers and Herculase:

Q5 ZraI forward primer: GTCCGGAGACTCTAGCGAGCGCCGGAGTATAAATAG

Q5 ZraI reverse primer: GTCACCTGCAGGCATGCGAATTCCACCTGCTTCAG

AseI and XbaI were used to remove the 8x QUAS from the QF2 QUAS E1B NLS Cardinal construct. The fragment was gel isolated, filled in using Klenow fragments, and cloned into the blunt 1GCT plasmid to give an 8x QUAS construct.

In vivo **Fluorescence Microscopy**

To begin, three-day-old larvae (three days after egg hatches) were selected from a food cap and fixed on a microscope slide containing a dried pad of 3% agar. In selecting the larvae,

larvae that were not expressing the tubby phenotype were selected because this ensured that they had the desired genes and therefore would express the necessary proteins. The larvae were then cleaned with water and mounted on a microscope slide with a coverslip taped to the slide to secure it. Oil was placed on top of the coverslip over the larva for use with the oil objective.

Both a Zeiss LSM 800 Upright and a Zeiss LSM 800 Inverted were used for experimentation, with the Upright microscope being used for both γ-tubulin and clathrin imaging. Zen software was used in conjunction with these microscopes to take and process images. The Zeiss LSM 800 Inverted microscope was used only for the clathrin experiments as it involved axotomy. On both of these microscopes, larvae were first located using the 10x objective, and all larvae were then imaged under the 63x oil objective. Images were taken only in larval segments A5, A4, and A3, or the 4^{th}, 5^{th}, and 6^{th} segments respectively counting from the larval tail [63]. Some images were taken in larval segment A6, or the 3^{rd} segment towards the beginning of my time in the lab, however, this was rectified as I progressed. All assays included the use of an RFP cell-shape marker to identify the presence of the neuron under the microscope. In γ-tubulin experiments, a membrane marker mCD8-RFP was used, and EB1-RFP was utilized in a clathrin experiment. At times, a membrane marker was not specifically needed due to strong expression of the protein of interest, which allowed for clear visualization of the neurons. After images were taken, the larvae were disposed of.

The images for γ-tubulin experiments were in the format of a Z stack, and the stack transitioned through various focal stages so that once the final image was taken, every part of the neuron was in focus at one point during the session. The Z stacks of one neuron were overlayed with maximum projection using ImageJ software for a clearer image and were used in data analysis. An overview Z stack was often taken in addition to a cropped Z stack that zoomed in on

particular branch points, specifically the 2nd through 5th branch points from the cell body. Data for clathrin experiments was also collected in this format.

Clathrin experiments also included video assays conducted by taking one large time series (150 slices) that focused on one or two specific branch points. The focus of these branch points was maintained for the entirety of the imaging session so that the movement of the clathrin puncta could be assessed. Additionally, both overview and zoomed images were taken in clathrin-related experiments investigating the behavior of other nucleation proteins when endocytosis was disrupted. For these experiments, larvae that were 3 or 4 days old were used.

For dsh localization experiments, larvae that were 3 or 4 days old were used.

Axon Injury

To sever axons expressing RFP membrane markers, I used the Zeiss LSM 800 inverted microscope and cut the axon using Oxford Instruments' MicroPoint laser. I cut class I ddaE axons proximally to the cell body, about halfway between the cell body and where the axon runs parallel to the ddaD axon. I then stored injured larvae at room temperature until imaging them eight hours later. I ensured successful cutting of the axon visually during imaging, or in some cases by an increased number of EB1 comets as is characteristic after axon injury [7].

Utilizing Shibire^{ts1} Heat Shock Mutants

I used the shibire^{ts1} temperature-sensitive mutant for experiments requiring disruption of clathrin-mediated endocytosis. Because this mutation is activated at temperatures as low as 29°C [61], I raised stocks of this line and crosses involving this line at 20°C to prevent induction of the

mutation during line or cross maturation. This gene resides on the X chromosome [60], so only male progeny of crosses express the mutant phenotype and therefore needed to be isolated.

Within *Drosophila*, shibire is the homolog for dynamin [59], which is involved in pinching off clathrin-coated vesicles from the cell membrane [33]. This mutant is unique in that it is temperature-sensitive, meaning that the mutation can be induced at any time by exposing the larvae to high temperatures, specifically 29°C, and when this mutation has been successfully induced, the larvae are paralyzed [61]. At a molecular level, this mutation targets dynamin and prevents it from folding correctly at high temperatures, and the result is disrupted clathrin-mediated endocytosis, as evidenced by the accumulation of unreleased clathrin-coated vesicles at the cell surface upon mutation induction [62].

Experimentation with this line involved two heat shocks, the first to identify male larvae expressing the mutation and the second to induce the heat shock immediately prior to imaging. The experimental setup was as follows. I put third instar larvae from crosses together onto a small slice of food inside of a covered food cap and incubated it at 37°C for 15 minutes to identify paralyzed male larvae prior to experimentation. After this first incubation, I placed paralyzed larvae into a food cap separate from larvae that had retained movement abilities. I stored these separated larvae at 20°C for 2-10 hours to allow sufficient recovery from the heat shock. After this time had passed, I placed a previously identified male and female larvae into a new food cap and incubated them at 37°C to re-induce the heat shock. The amount of time of this second heat shock was either 15 minutes or 30 minutes depending on the experiment. Gonads are visible as two translucent circles proximal to the larval posterior end, and I used this characteristic as another checkpoint to ensure that paralyzed larvae were indeed males and that males therefore were successfully expressing the mutation (**Fig 15**).

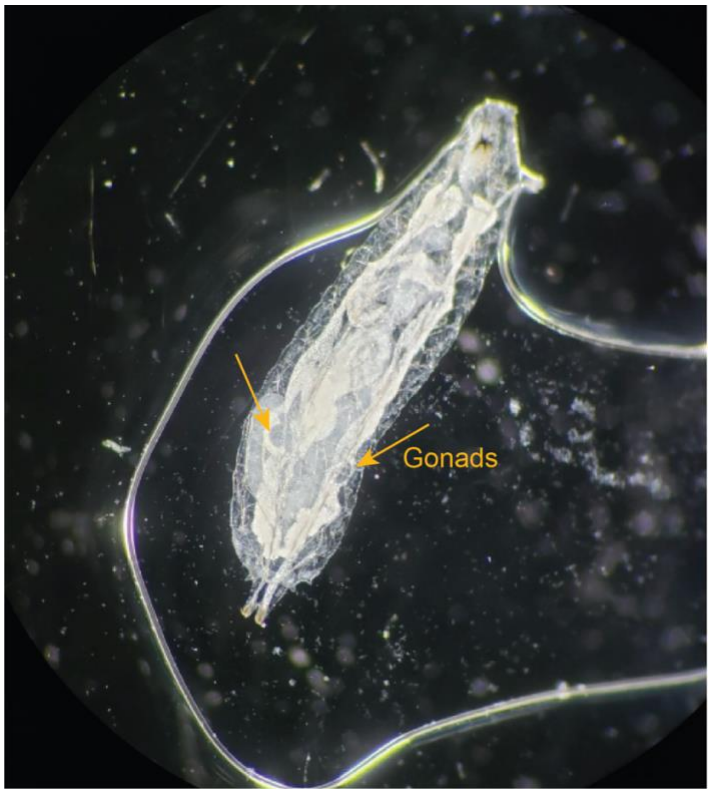

Figure 15: Identification of Gonads in Male Larva. Male larvae are distinguishable by the presence of gonads, which appear after compression of larva under a microscope cover slip. They appear as two translucent circles near the posterior end.

In addition to inducing the heat shock via incubation, I used an objective heating collar to warm the 63x objective to between 34 and 37°C to ensure maintenance of the temperature-sensitive mutation (**Fig 16**). I also gave the control crosses for these experiments the same treatment in terms of storage temperature and heat shock induction to promote consistency between control and experimental groups. Lines involved in control crosses were the tester line for the protein of interest crossed with yellow white (yw). However, I did not screen larvae of control crosses for paralysis or try to identify gonads since no X-linked mutation was present in lines used in control experiments. It is unlikely that there are any sex-specific differences in larvae because they are not sexually mature, and in my experiments thus far, I have not seen any

sex-specific differences. But, these potential differences may be something to consider in future experiments.

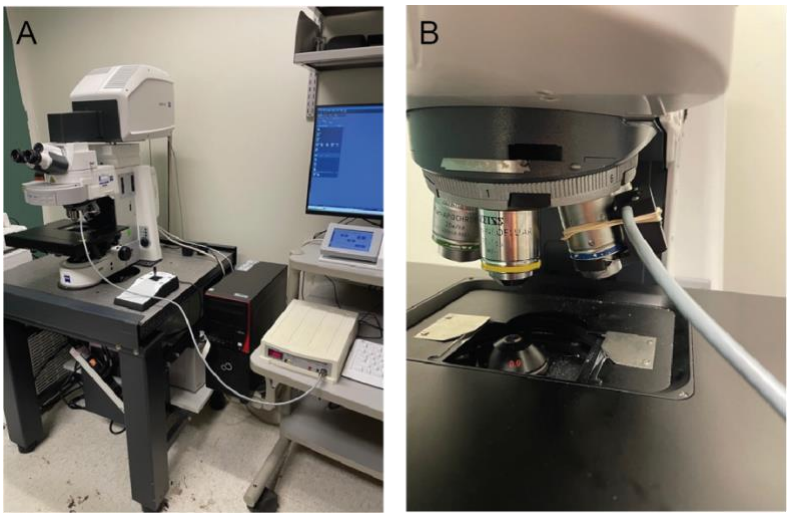

Figure 16: Objective Heating Collar During Experiment. An objective heating collar connected to a heating element was attached to the 63x objective during experimentation to ensure that the mutant larvae did not recover from the heat shock during imaging. The collar was set to heat to 37°C.

Initially, I had used female larvae to collect the control data set since they did not express the temperature-sensitive mutation due to having a wildtype X chromosome. However, identifying male gonads, or lack thereof, started to become ambiguous because I started to see some larvae that had maintained movement abilities but also appeared to have gonads. I developed two solutions to effectively solve this problem. In the first, I saved larvae that I had imaged that had maintained mobility in individual vials and let them reach adulthood, where males and females have more distinguished anatomical differences. However, none of the larvae I saved advanced past pupation in both 20°C or 25°C storage. Another approach I came up with involved crossing the tester line of the protein of interest to yellow-white (yw) instead of shibire. I then used larvae from this cross, regardless of sex, for my control data set. None of these lines have their genes of interest expressed on X, so there is no need to distinguish between male and

female larvae. This removes the ambiguity in identifying the control specimens and ensures with certainty that control larvae do not express the temperature-sensitive mutation.

Quantifications for γTub Fluorescence Intensity at Dendritic Branch Points

Images were processed to maximum projection z-stacks. However, some images may have been analyzed as average intensity z-stacks for this data set as I was only beginning to learn the software. This does not change the conclusion that a new skin cell tester line is needed as background interference is still evident in the images. To determine fluorescence intensity, each branch point of the comb dendrite was outlined and the average fluorescence intensity of that region was obtained. In an attempt to subtract background interference from epithelial cells, a region adjacent to the neuron was outlined and the average fluorescence intensity of that region was also obtained. This effort was not useful as the varying background interference was not consistent along the length of the neuron. No statistical analyses were performed due to this background interference.

Quantifications of Clathrin Puncta Characteristics

Clathrin videos were used for this analysis. Adjustments using ImageJ included using the template matching plugin to align slices in the case that the animal moved during imaging. Branch points that were in focus for the entirety of the video were used, and branch points with distinct puncta cycling within the branch point region were marked as containing moving puncta. Puncta within each branch point were marked as stationary if they did not cycle within the branch point region. Statistical significance was determined using a Fisher's exact test for puncta

mobility and an unpaired *t* test for the stationary puncta per branch point. For both tests, * p-value <0.05, ** p-value <0.01, and *** p-value <0.001.

Quantifications of Dsh Puncta Intensity

Images were processed to maximum projection z-stacks. Additional adjustments using ImageJ included using the template matching plugin to align slices in the case that the animal moved during imaging. Only the puncta visible at 75% zoom in ImageJ were included in the analysis. To determine the maximum intensity of each punctum, each punctum was enlarged to 3200% in ImageJ, and the maximum intensity of each punctum was determined by hovering over each pixel within the punctum. Values were displayed on the ImageJ toolbar. Puncta were assigned to intensity categories based on their maximum intensities, and a Chi-square test was used to determine significance. P-values <0.05 were considered statistically significant.

Chapter 4

Discussion

With the skin cell tester line I had developed at the beginning of my involvement in this research (UAS-mCD8-RFP; UAS-γTub-GFP, A58-Gal4), I was unable to determine if inhibiting Wnt secretion impacted γTub localization at dendritic branch points (**Fig 9**). This was because of the high amount of background interference arising from γTub expression in the nearby epithelial cells. As a result, I began making a new skin cell tester line that would use two different transcription systems so that expression in the neurons and in the epithelial cells were regulated individually, which would allow for expression of γTub only in the neurons of interest (**Fig 10**). I began working with our lab's molecular biologist to create this new line. However, I was unable to finish due to the Covid-19 pandemic. In my absence, the line was completed to give the new skin cell tester line (QUAS-γTub-GFP, QUAS-myr-tdtomato, TMC-QF/Cyo; A58-gal4, dicer2-nLS-BFP/TM6) (**Fig 11**). Future studies include using this new tester line in conjunction with RNAis targeting wntless and other Wnt-specific genes to determine the effect of epithelial Wnts on γTub localization. Pankajam Thyagarajan, a graduate student in Dr. Rolls' lab, has been continuing this portion of the project.

Because of the delayed development of this line, I shifted my focus to investigating the more upstream portion of how previously identified Wnt signaling proteins localized to Rab5-coated endosomes [25] enter the cell in order to mediate γTub localization and subsequent MT nucleation at dendritic branch points. I first began by characterizing the behavior of clathrin at the dendritic branch points both in a normal animal and when clathrin-mediated endocytosis was inhibited with the use of the shibire^{ts1} temperature-sensitive mutant (**Fig 12**). At dendritic branch points of class I neurons, clathrin forms puncta that either remain stationary or cycle within the

branch point, and we suspect that these puncta are inside of the cell because of their movement behaviors. When clathrin-mediated endocytosis is inhibited, there are fewer branch points with mobile clathrin puncta, which makes sense given that induction of the mutation in shi^{ts1} mutants arrests clathrin-coated vesicles at the cell surface, preventing the completion of endocytosis [62]. However, there was no difference in the number of stationary puncta in wildtype and shibire mutant animals. Future investigation regarding the behavior of clathrin puncta includes using tracking software to track and measure the movement of each mobile punctum to determine if there are differences in movement patterns, velocities, etc. within the branch points.

I also investigated the impact that axon injury has on the behavior of clathrin (**Fig 14**). After axon injury, EB1 comets are upregulated [7], indicating that there is an increase in MT nucleation. I hypothesized that if clathrin-mediated endocytosis is involved upstream of γTub localization, the activity of clathrin should also be upregulated after axon injury. In measuring the same mobility parameters as in the baseline assay, I did see an increase in the percentage of branch points containing mobile clathrin puncta, however, this was not a significant difference. One of my current experiments involves increasing the sample size to determine if that effect becomes more pronounced.

Finally, I investigated the impact that inhibiting clathrin-mediated endocytosis has on the levels of dsh present at dendritic branch points (**Fig 13**) in an effort to determine how clathrin-mediated endocytosis influences Wnt signaling. Dsh (named Dvl in other organisms) is a key Wnt signaling protein that localizes to the plasma membrane [31] to aid in Fz/LRP6 receptor oligomerization [27] and axin recruitment [27], [31]. After a 15-minute heat shock immediately prior to imaging, there was no difference in the amount of dsh present at dendritic branch points between the wildtype and mutant conditions, indicating that clathrin-mediated endocytosis may

not play a role in wnt signaling. However, it could be that endocytosis was not arrested long enough to produce a noticeable phenotype. Another of my current experiments includes incubating larvae for 45 minutes immediately prior to imaging followed by the same imaging and analysis techniques to determine if there is a more noticeable phenotype. Additional experiments in this area include investigating the impact of clathrin-mediated endocytosis inhibition on levels of other proteins such as Axin, γTub, and Rab5. Another direction would be to look at the colocalization of dsh and the aforementioned proteins with clathrin. Finally, in experiments involving the shibire mutant, sex-specific differences should be taken into account and explored.

Neurons are crucial to the survival and function of every organism, as is evident in the development of neurodegenerative diseases when the activity of these neurons deviates from the norm. Uncovering the mechanisms underlying the organization and structure of neurons is therefore essential and could provide the foundation for new treatments targeting these diseases.

References

[1] K. J. T. Venken and H. J. Bellen, “Emerging technologies for gene manipulation in Drosophila melanogaster,” *Nature Reviews Genetics*. 2005, doi: 10.1038/nrg1553.

[2] L. T. Reiter, L. Potocki, S. Chien, M. Gribskov, and E. Bier, “A systematic analysis of human disease-associated gene sequences in Drosophila melanogaster,” *Genome Res.*, 2001, doi: 10.1101/gr.169101.

[3] A. Singhania and W. B. Grueber, “Development of the embryonic and larval peripheral nervous system of Drosophila,” *Wiley Interdiscip. Rev. Dev. Biol.*, 2014, doi: 10.1002/wdev.135.

[4] R. Bodmer and Y. N. Jan, “Morphological differentiation of the embryonic peripheral neurons in Drosophila,” *Roux’s Arch. Dev. Biol.*, 1987, doi: 10.1007/BF00402027.

[5] W. B. Grueber, L. Y. Jan, and Y. N. Jan, “Tiling of the Drosophila epidermis by multidendritic sensory neurons,” *Development*, 2002.

[6] M. M. Nguyen *et al.*, “γ-tubulin controls neuronal microtubule polarity independently of Golgi outposts,” *Mol. Biol. Cell*, 2014, doi: 10.1091/mbc.E13-09-0515.

[7] M. C. Stone, M. M. Nguyen, J. Tao, D. L. Allender, and M. M. Rolls, “Global Up-Regulation of Microtubule Dynamics and Polarity Reversal during Regeneration of an Axon from a Dendrite,” *Mol. Biol. Cell*, vol. 21, pp. 767–777, 2010, doi: 10.1091/mbc.E09.

[8] L. C. Kapitein and C. C. Hoogenraad, “Building the Neuronal Microtubule Cytoskeleton,” *Neuron*, vol. 87, no. 3, pp. 492–506, Aug. 2015, doi: 10.1016/J.NEURON.2015.05.046.

[9] N. Hirokawa, S. Niwa, and Y. Tanaka, “Molecular motors in neurons: Transport mechanisms and roles in brain function, development, and disease,” *Neuron*, vol. 68, no. 4, pp. 610–638, Nov. 2010, doi: 10.1016/J.NEURON.2010.09.039.

[10] J. R. Kardon and R. D. Vale, “Regulators of the cytoplasmic dynein motor,” *Nat. Rev. Mol. Cell Biol. 2009 1012*, vol. 10, no. 12, pp. 854–865, Dec. 2009, doi: 10.1038/nrm2804.

[11] H. Zempel and E.-M. Mandelkow, “Linking Amyloid-β and Tau: Amyloid-β Induced Synaptic Dysfunction via Local Wreckage of the Neuronal Cytoskeleton,” *Neurodegener. Dis.*, vol. 10, no. 1–4, pp. 64–72, Apr. 2012, doi: 10.1159/000332816.

[12] J. Dubey, N. Ratnakaran, and S. P. Koushika, “Neurodegeneration and microtubule dynamics: death by a thousand cuts,” *Front. Cell. Neurosci.*, vol. 0, no. September, p. 343, Sep. 2015, doi: 10.3389/FNCEL.2015.00343.

[13] A. J. Matamoros and P. W. Baas, “Microtubules in health and degenerative disease of the nervous system,” *Brain Res. Bull.*, vol. 126, pp. 217–225, Sep. 2016, doi: 10.1016/j.brainresbull.2016.06.016.

[14] J. Howard and A. A. Hyman, “Growth, fluctuation and switching at microtubule plus ends,” *Nat. Rev. Mol. Cell Biol. 2009 108*, vol. 10, no. 8, pp. 569–574, Jun. 2009, doi: 10.1038/nrm2713.

[15] A. Akhmanova and M. O. Steinmetz, “Tracking the ends: a dynamic protein network controls the fate of microtubule tips,” *Nat. Rev. Mol. Cell Biol. 2008 94*, vol. 9, no. 4, pp. 309–322, Apr. 2008, doi: 10.1038/nrm2369.

[16] C. A. Tovey and P. T. Conduit, “Microtubule nucleation by γ-tubulin complexes and beyond,” *Essays in Biochemistry*. 2018, doi: 10.1042/EBC20180028.

[17] S. E. Hill *et al.*, “Development of dendrite polarity in Drosophila neurons,” *Neural Dev. 2012 71*, vol. 7, no. 1, pp. 1–13, Oct. 2012, doi: 10.1186/1749-8104-7-34.

[18] J. M. Kollman, A. Merdes, L. Mourey, and D. A. Agard, “Microtubule nucleation by γ-tubulin complexes,” *Nat. Rev. Mol. Cell Biol.*, vol. 12, no. 11, pp. 709–721, 2011, doi: 10.1038/nrm3209.

[19] D. Job, O. Valiron, and B. Oakley, “Microtubule nucleation,” *Curr. Opin. Cell Biol.*, vol. 15, no. 1, pp. 111–117, 2003, doi: 10.1016/S0955-0674(02)00003-0.

[20] A. Leask, K. Obrietan, and T. Stearns, “Synaptically coupled central nervous system neurons lack centrosomal γ-tubulin,” *Neurosci. Lett.*, vol. 229, no. 1, pp. 17–20, Jun. 1997, doi: 10.1016/S0304-3940(97)00412-6.

[21] M. M. Nguyen, M. C. Stone, and M. M. Rolls, “Microtubules are organized independently of the centrosome in Drosophila neurons,” *Neural Dev.*, 2011, doi: 10.1186/1749-8104-6-38.

[22] T. Consolati *et al.*, “Microtubule Nucleation Properties of Single Human γTuRCs Explained by Their Cryo-EM Structure,” *Dev. Cell*, vol. 53, no. 5, pp. 603-617.e8, Jun. 2020, doi: 10.1016/J.DEVCEL.2020.04.019.

[23] G. J. Brouhard *et al.*, “XMAP215 Is a Processive Microtubule Polymerase,” *Cell*, vol. 132, no. 1, pp. 79–88, Jan. 2008, doi: 10.1016/J.CELL.2007.11.043.

[24] A. T. Weiner, P. Thyagarajan, Y. Shen, and M. M. Rolls, “To nucleate or not, that is the question in neurons,” *Neurosci. Lett.*, vol. 751, p. 135806, Apr. 2021, doi: 10.1016/J.NEULET.2021.135806.

[25] A. T. Weiner *et al.*, “Endosomal Wnt signaling proteins control microtubule nucleation in dendrites,” *PLoS Biol.*, vol. 18, no. 3, 2020, doi: 10.1371/journal.pbio.3000647.

[26] L. Brunt and S. Scholpp, “The function of endocytosis in Wnt signaling,” *Cell. Mol. Life Sci.*, vol. 75, no. 5, p. 785, Mar. 2018, doi: 10.1007/S00018-017-2654-2.

[27] K. M. Cadigan and M. Peifer, “Wnt signaling from development to disease: insights from model systems,” *Cold Spring Harb. Perspect. Biol.*, vol. 1, no. 2, 2009, doi: 10.1101/CSHPERSPECT.A002881.

[28] G. Davidson *et al.*, “Casein kinase 1 gamma couples Wnt receptor activation to cytoplasmic signal transduction,” *Nature*, vol. 438, no. 7069, pp. 867–872, Dec. 2005, doi: 10.1038/NATURE04170.

[29] V. L. Katanaev, R. Ponzielli, M. Sémériva, and A. Tomlinson, “Trimeric G Protein-Dependent Frizzled Signaling in Drosophila,” *Cell*, vol. 120, no. 1, pp. 111–122, Jan. 2005, doi: 10.1016/J.CELL.2004.11.014.

[30] A. Koval, V. Purvanov, D. Egger-Adam, and V. L. Katanaev, “Yellow submarine of the Wnt/Frizzled signaling: Submerging from the G protein harbor to the targets,” *Biochem. Pharmacol.*, vol. 82, no. 10, pp. 1311–1319, Nov. 2011, doi: 10.1016/J.BCP.2011.06.005.

[31] C. Gao and Y. G. Chen, “Dishevelled: The hub of Wnt signaling,” *Cell. Signal.*, vol. 22, no. 5, pp. 717–727, May 2010, doi: 10.1016/J.CELLSIG.2009.11.021.

[32] L. Chen, M. C. Stone, J. Tao, and M. M. Rolls, “Axon injury and stress trigger a microtubule-based neuroprotective pathway,” *Proc. Natl. Acad. Sci. U. S. A.*, vol. 109, no. 29, pp. 11842–11847, Jul. 2012, doi: 10.1073/PNAS.1121180109/-/DCSUPPLEMENTAL.

[33] M. Kaksonen and A. Roux, “Mechanisms of clathrin-mediated endocytosis,” *Nat. Rev. Mol. Cell Biol. 2018 195*, vol. 19, no. 5, pp. 313–326, Feb. 2018, doi: 10.1038/nrm.2017.132.

[34] Y. C. Wu, Y. C. Chiang, S. H. Chou, and C. L. Pan, “Wnt signalling and endocytosis: Mechanisms, controversies and implications for stress responses,” *Biol. Cell*, vol. 113, no. 2, pp. 95–106, Feb. 2021, doi: 10.1111/BOC.202000099.

[35] “What is clathrin-mediated endocytosis? | MBInfo.” https://www.mechanobio.info/what-is-the-plasma-membrane/what-is-membrane-trafficking/what-is-clathrin-mediated-endocytosis/ (accessed Mar. 18, 2022).

[36] I. Kim, W. Pan, S. A. Jones, Y. Zhang, X. Zhuang, and D. Wu, “Clathrin and AP2 are required for PtdIns(4,5)P2-mediated formation of LRP6 signalosomes,” *J. Cell Biol.*, vol. 200, no. 4, pp. 419–428, Feb. 2013, doi: 10.1083/JCB.201206096.

[37] A. I. H. Hagemann *et al.*, “In vivo analysis of formation and endocytosis of the Wnt/β-Catenin signaling complex in zebrafish embryos,” *J. Cell Sci.*, vol. 127, no. 18, pp. 3970–3982, 2014, doi: 10.1242/JCS.148767/-/DC1.

[38] E. S. Seto and H. J. Bellen, “Internalization is required for proper Wingless signaling in Drosophila melanogaster,” *J. Cell Biol.*, vol. 173, no. 1, p. 95, Apr. 2006, doi: 10.1083/JCB.200510123.

[39] M. Zerial and H. McBride, “Rab proteins as membrane organizers,” *Nat. Rev. Mol. Cell Biol. 2001 22*, vol. 2, no. 2, pp. 107–117, Feb. 2001, doi: 10.1038/35052055.

[40] C. A. Worby and J. E. Dixon, “Sorting out the cellular functions of sorting nexins,” *Nat. Rev. Mol. Cell Biol. 2002 312*, vol. 3, no. 12, pp. 919–931, Dec. 2002, doi: 10.1038/nrm974.

[41] L. Sun, X. Hu, W. Chen, W. He, Z. Zhang, and T. Wang, “Sorting nexin 27 interacts with Fzd7 and mediates Wnt signalling,” *Biosci. Rep.*, vol. 36, no. 1, p. 296, Feb. 2016, doi: 10.1042/BSR20150205.

[42] Y. Jiang, X. He, and P. H. Howe, “Disabled-2 (Dab2) inhibits Wnt/β-catenin signalling by binding LRP6 and promoting its internalization through clathrin,” *EMBO J.*, vol. 31, no. 10, pp. 2336–2349, May 2012, doi: 10.1038/EMBOJ.2012.83.

[43] D. Wu and W. Pan, “GSK3: a multifaceted kinase in Wnt signaling,” *Trends Biochem. Sci.*, vol. 35, no. 3, p. 161, Mar. 2010, doi: 10.1016/J.TIBS.2009.10.002.

[44] J. Z. Parrish, P. Xu, C. C. Kim, L. Y. Jan, and Y. N. Jan, “The microRNA bantam Functions in Epithelial Cells to Regulate Scaling Growth of Dendrite Arbors in Drosophila Sensory Neurons,” *Neuron*, vol. 63, no. 6, pp. 788–802, Sep. 2009, doi: 10.1016/J.NEURON.2009.08.006.

[45] Y. Wang, H. Wang, X. Li, and Y. Li, “Epithelial microRNA-9a regulates dendrite growth through Fmi-Gq signaling in Drosophila sensory neurons,” *Dev. Neurobiol.*, vol. 76, no. 2, pp. 225–237, Feb. 2016, doi: 10.1002/DNEU.22309.

[46] Y. Yuva-Aydemir, A. Simkin, E. Gascon, and F. B. Gao, “MicroRNA-9: functional evolution of a conserved small regulatory RNA,” *RNA Biol.*, vol. 8, no. 4, 2011, doi: 10.4161/RNA.8.4.16019.

[47] T. Usui *et al.*, “Flamingo, a seven-pass transmembrane cadherin, regulates planar cell polarity under the control of Frizzled,” *Cell*, vol. 98, no. 5, pp. 585–595, Sep. 1999, doi: 10.1016/S0092-8674(00)80046-X.

[48] C. Han *et al.*, “Epidermal cells are the primary phagocytes in the fragmentation and clearance of degenerating dendrites in Drosophila,” *Neuron*, vol. 81, no. 3, p. 544, Feb. 2014, doi: 10.1016/J.NEURON.2013.11.021.

[49] L. Luo and D. D. M. O’Leary, “Axon retraction and degeneration in development and disease,” *Annu. Rev. Neurosci.*, vol. 28, pp. 127–156, 2005, doi:

10.1146/ANNUREV.NEURO.28.061604.135632.

[50] D. W. Williams and J. W. Truman, “Cellular mechanisms of dendrite pruning in Drosophila: insights from in vivo time-lapse of remodeling dendritic arborizing sensory neurons,” *Development*, vol. 132, no. 16, pp. 3631–3642, Aug. 2005, doi: 10.1242/DEV.01928.

[51] S. Hall, “The response to injury in the peripheral nervous system,” *J. Bone Jt. Surg. - Ser. B*, vol. 87, no. 10, pp. 1309–1319, Oct. 2005, doi: 10.1302/0301-620X.87B10.16700/ASSET/IMAGES/LARGE/16700-4.JPEG.

[52] T. C. Frank-Cannon, L. T. Alto, F. E. McAlpine, and M. G. Tansey, “Does neuroinflammation fan the flame in neurodegenerative diseases?,” *Mol. Neurodegener.*, vol. 4, no. 1, p. 47, 2009, doi: 10.1186/1750-1326-4-47.

[53] S. Meltzer *et al.*, “Epidermis-Derived Semaphorin Promotes Dendrite Self-Avoidance by Regulating Dendrite-Substrate Adhesion in Drosophila Sensory Neurons,” *Neuron*, 2016, doi: 10.1016/j.neuron.2016.01.020.

[54] N. Jiang *et al.*, “A conserved morphogenetic mechanism for epidermal ensheathment of nociceptive sensory neurites,” *Elife*, 2019, doi: 10.7554/eLife.42455.

[55] “FlyBase Gene Report: Dmel\wls.” https://flybase.org/reports/FBgn0036141 (accessed Mar. 17, 2022).

[56] E. Giniger, S. M. Varnum, and M. Ptashne, “Specific DNA binding of GAL4, a positive regulatory protein of yeast,” *Cell*, vol. 40, no. 4, pp. 767–774, 1985, doi: 10.1016/0092-8674(85)90336-8.

[57] O. Riabinina and C. J. Potter, “The q-system: A versatile expression system for drosophila,” in *Methods in Molecular Biology*, 2016.

[58] A. H. Brand and N. Perrimon, “Targeted gene expression as a means of altering cell fates and generating dominant phenotypes,” *Development*, 1993.

[59] “FlyBase Gene Report: Dmel\shi.” https://flybase.org/reports/FBgn0003392.html (accessed Feb. 22, 2022).

[60] “FlyBase Allele Report: Dmel\shi[1].” https://flybase.org/reports/FBal0015610.html (accessed Sep. 29, 2021).

[61] T. A. Grigliatti, L. Hall, R. Rosenbluth, and D. T. Suzuki, “Temperature-Sensitive Mutations in Drosophila melanogaster XIV. A Selection of Immobile Adults *,” 1973.

[62] T. Kosaka and K. Ikeda, “Possible temperature-dependent blockage of synaptic vesicle recycling induced by a single gene mutation in drosophila,” *J. Neurobiol.*, vol. 14, no. 3, pp. 207–225, 1983, doi: 10.1002/NEU.480140305.

[63] S. B. M. Gowda, S. Salim, and F. Mohammad, “Anatomy and Neural Pathways Modulating Distinct Locomotor Behaviors in Drosophila Larva,” *Biol. 2021, Vol. 10, Page 90*, vol. 10, no. 2, p. 90, Jan. 2021, doi: 10.3390/BIOLOGY10020090.

MELISSA LONG

EDUCATION

The Pennsylvania State University, University Park, PA — Anticipated Graduation: May 2022
Bachelor of Science: *Immunology and Infectious Disease*
Honors: Schreyer Honors College, Academic Excellence Scholarship, Dean's List
Relevant Coursework: Epidemiology, Immunology, Sociology, Spanish

EXPERIENCE

Dr. Melissa Rolls Lab, University Park, PA — 2019 - Present
Undergraduate Researcher

- Investigate principles of neuronal regeneration and function in the model system *Drosophila*
- Design experiments with thorough consideration of confounding variables
- Analyze experimental results to form conclusions and apply them to overarching scientific field
- Collaborate with experienced scientists to promote project guidance and comprehension
- Communicate detailed concepts to a general audience through strategically designed figures
- Train and support new undergraduate researchers

Willow Valley Communities, Willow Street, PA — 2016 - 2021
Dining Server and Culinary Mentor

- Served meals to elderly residents to ensure quality customer service and care
- Established meaningful relationships with residents
- Trained new servers in preparation for workplace independence

LEADERSHIP AND COMMUNITY SERVICE

State College Alliance Church, State College, PA
Conversational English Class Volunteer — Fall 2021 - Present

- Assisted in development of conversational English class program for internationals
- Promoted program awareness within the surrounding community

The Navigators at Penn State, University Park, PA — August 2018 – Present
Bible Study Leader — Fall 2019 – Present

- Lead weekly Bible studies and facilitate discussion
- Promote community development amongst Penn State students
- Provide one-on-one mentorship to students

Service Trip Laborer, New Bern, NC and Philadelphia, PA — Spring 2019, 2020

- Rebuilt hurricane-damaged homes with Baptists on Mission
- Performed maintenance duties at Roxborough Church and local homeless shelters
- Partnered with The Philadelphia Project for community outreach

Leadership Development Program Trainee, St. Petersburg, FL — Summer 2019

- Engaged in leadership workshops to advance interpersonal skills
- Implemented organizational principles in the community

TECHNICAL SKILLS

- **Proficient with:** Microsoft Office Suite, Adobe Illustrator
- **Conversationally Fluent in:** Spanish